The sound of plastic

A proof-of-concept for detecting suspended riverine macroplastics with echo sounding

by Sophie Broere

TUDelft

The sound of plastic
A proof-of-concept for detecting suspended riverine macroplastics with echo sounding

By

Sophie Broere

in partial fulfilment of the requirements for the degree of

Master of Science
in Civil Engineering

at the Delft University of Technology,
to be defended publicly on Wednesday April 8, 2020 at 12:00.

Thesis committee:	Prof. dr. ir. N.C. van de Giesen	TU Delft (Chair)
	Ir. W.M.J. Luxemburg	TU Delft
	Dr. ir. M.A. de Schipper	TU Delft
	Dr. ir. T.H.M. van Emmerik	Wageningen University
	Dr. D. Gonzáles-Fernández	University of Cádiz

ŤUDelft

Preface

In this master thesis, the use of echo sounding for riverine macroplastics monitoring is explored. I experienced my thesis research as very interesting and challenging and I am proud of the result. This thesis was the final project concerning my Water Resources Management master at the Delft University of Technology.

First of all, I would like to thank Wim. You made me come up with my own master research topic, were always approachable to have a chat (not only about my research) and supported me during my masters at the Water Resources department. Secondly, Tim, thank you for providing me with the necessary insight into the current state of plastic research and guiding me throughout my thesis project. During my fieldwork in Cádiz, Southern Spain, I had the pleasure to meet Daniel and Andrés. Thank you both for your assistance and enthusiasm, I really enjoined my time in Cádiz. Nick and Matthieu thank you for your suggestions, time and objective judgements.

Furthermore, I would like to thank Gavin ten Tusscher for carefully reading and commenting on my report. Lastly, thanks to my family and friends who motivated and supported me during my study career at the TU Delft.

Sophie Broere
Delft, April 2020

Summary

Plastic pollution in aquatic ecosystems is a global problem. Rivers transport large quantities of litter from land to the oceans. Plastics of different sizes and properties are widely present at various locations in river systems. Concerning macroplastics, previous studies mainly focussed on floating plastics, however, substantial parts of the litter can be transported underneath the water surface. Currently, this suspended litter load remains understudied. Submerged litter is presently monitored with the use of nets. The use of nets has several disadvantages. In large rivers, nets can usually, not be deployed over the full depth and width of the river. Moreover, using nets is labour intensive and requires fixed structures to be deployed. To overcome this problem, this thesis aimed to develop and test a new method for monitoring submerged riverine litter. In accordance with the fish detection abilities of sonar, it seems to have a high potential for identifying suspended underwater objects.

In this study, the litter detection ability of a low-cost single beam echosounder (Deeper CHIRP+) were investigated. Three different experiments were executed, in specific, controlled tests in an artificial environment, semi-controlled tests in a natural environment and litter monitoring in a naturally flowing river. The controlled tests, to get an insight into the scanning technique and detection abilities of the echosounder, were performed in the Kerkpolderbad in Delft. During these tests, the influence of actual object size, object depth and flow velocity on the sonar signal was investigated. The semi-controlled tests were carried out in the Rio de San Pedro, in Andalusia, Southern Spain. During these tests, several plastic targets were used and repeatedly released in the river, passing the sensor. For this, objects of different material properties and sizes were used. Lastly, plastic was monitored in the Guadalquivir and Guadalete rivers in Andalusia. In the Guadalquivir river, the sensor was operated together with nets for validation purposes. In the Guadalete river, monitoring took place for 18 hours from a pedestrian bridge, at different locations over the cross-section of the river and under varying tidal conditions.

The performed tests showed a significant relationship between the dimensions of the reflection signal, derived from the sonar observations and the actual object size. However, object orientation and deformation play a role and lead to deviations in the signal dimension results. A second relation, regarding flow velocity and signal dimensions, was observed. The larger the flow velocity, the smaller the sonar signal. Additionally, signal intensities can, for four out of the eight objects tested, be related to material properties but differences in signal intensities are relatively small. Regarding the river monitoring activities, suspended litter items can be counted, river tide is influencing litter transport and litter is present over the full river depth.

The following main conclusions are drawn based on this research:
- ❖ Echo sounding can be used for detecting suspended riverine macroplastics. Litter items can be counted, and fish can be discarded from the sonar readings by their specific displayed shapes.
- ❖ Litter size can be estimated when looking at the sonar readings, however, several factors, such as flow velocity, object orientation and deformation have to be taken into account when estimating litter size.
- ❖ In the Guadalete river, significantly more suspended litter is transported when river water flows into the sea compared to river water flowing inland. The counted litter items were approximately uniformly distributed over the river depth.

In general, using echo sounding for suspended litter monitoring is potentially useful to gain a better understanding of the suspended litter transport, from which prevention and mitigation strategies could be optimised. For further research, it is recommended to use an echosounder for which the raw sonar data can be exported as a standard digital file. Moreover, the set of test objects should be extended, including more variation in object size. To separate signal size and signal intensity, objects of different size but same material properties and objects of the same size but different material properties should be used for testing. Finally, other types of sonar such as side scan or multibeam sonars may potentially lead to more accurate sonar readings regarding litter size and material estimations.

Contents

1.
Introduction

Plastic pollution is progressively present in the news. Media all over the world write about the presence and danger of plastics in the natural environment. Statements such as, 'By 2050, the oceans will contain more plastic than fish by weight' (MacArthur, 2016) and 'Even babies born pre-polluted' (Di Renzo et al., 2015), get worldwide attention, but can these statements be confirmed with the knowledge we have?

The plastic pollution problem is, in particular, caused by the disposal of single-use plastics. Single-use plastics are produced in large amounts and only used once before disposal. Due to low recycling rates, these plastics appear to end up in natural environments, as presented in Figure 1. To tackle this problem, the government of the European Union is changing the legislation where it comes to single-use plastics. By 2021, disposable single-use plastics, such as straws, forks, knives, plates, and cotton swabs, will be banned (European Parliament, 2019). Previously, in 2015 the policy on plastic bags had already been changed (European Parliament, 2015). The changed policy aimed at reducing the consumption of lightweight plastic carrier bags. It forbids shops to provide complimentary plastic bags. Still, the plastic pollution problem remains prevalent as plastics continue polluting our natural environments.

Figure 1: Seahorse with a cotton swab (Hofman, 2017).

In the field of scientific research, insight in to the presence, behaviour, and fate of plastics in our natural environments is steadily gained. However, information from research remains limited and a lot of questions are presently unanswerable. In this thesis, the focus is on getting insight into the transport of plastics underneath the water surface, by finding a method to continuously monitor submerged plastics. More information about this is provided in the coming sections.

In the remaining parts of this chapter, the specific problem and objectives, that are focussed on in this thesis, are stated. In section 1.1, the problem motivation is given. The problem statement is provided in section 1.2. From the problem motivation and problem statement follow the objectives addressed in this thesis, described in section 1.3. To narrow the field of research, the scope of this thesis is stated in section 1.4. Leading to the research questions, mentioned in section 1.5. In section 1.6, a short overview of the research method is given. Lastly, the outline of the report is specified in section 1.7.

1.1. Problem motivation

Over the last decades, worldwide plastic production increased has tremendously. From the 1950s to 2018, the plastic production expanded from 1.7 to 359 million metric tons per year (Tramoy et al., 2019); (PlasticsEurope, 2019). China is the largest producer of plastics, followed by Europe. In general, plastics are widely used because of their unique combination of low cost, light-weight, and durability (PlasticsEurope, 2018).

Although, plastics are widely used and integrated into our daily lives, not all plastic waste is sufficiently managed. This results in plastics ending up and persisting in the natural environment. Globally, the disposal of plastics into the oceans is estimated to be between 0.5 and 12.7 million tons each year (Jambeck et al., 2015). These plastics originate from sources on land as well as at sea (fishing industry), causing both severe global problems, regarding risks for human health and environmental- and economic damage (European Commission, 2018). Plastic waste causes contamination of the natural environment because of its persistence and tendency for fragmentation into microplastics (Schmidt et al., 2017). This may lead to animals getting entangled in plastics, animals ingesting plastics, leakage of toxic additives and adsorption of chemicals to plastic debris (van Emmerik & Schwarz, 2019). Furthermore, plastic waste induces overall damage to the human livelihood, involving economical damage regarding, for instance, tourism and recreation.

The major part of the plastic waste that ends up in the oceans is transported by rivers (Schmidt et al., 2017). According to Lebreton et al., (2017), it is estimated that yearly between 1.15 and 2.41 million tonnes of plastic waste enter the oceans via rivers. These global quantities are nonetheless associated with uncertainties due to methodological difficulties to accurately quantify land-based plastic fluxes into the ocean (Tramoy et al., 2019). Yet, there are no standard methods to determine quantities of plastics in rivers (González et al., 2016). Moreover, most research is focussed on marine litter instead of riverine litter, resulting in riverine litter being understudied (van Emmerik & Schwarz, 2019).

To reduce the amount of plastic waste in the natural environment, information on plastic fluxes from rivers to seas is needed (González et al., 2016). Additionally, focussing on the monitoring of plastic litter that is transported by rivers is useful because measures can easier be implemented in two-dimensional rivers than three-dimensional seas (Tramoy et al., 2019). Data on riverine litter fluxes can, for example, be used for determining locations for plastic reduction interventions.

In general, a distinction is made between plastics present at the river banks and in the water body. When it comes to litter in the river water body, there is a division in the vertical river profile, illustrated in Figure 2. At the water surface, there are floating litter objects present, in the water column litter objects are submerged. At the river bottom, plastics can be transported as bedload.
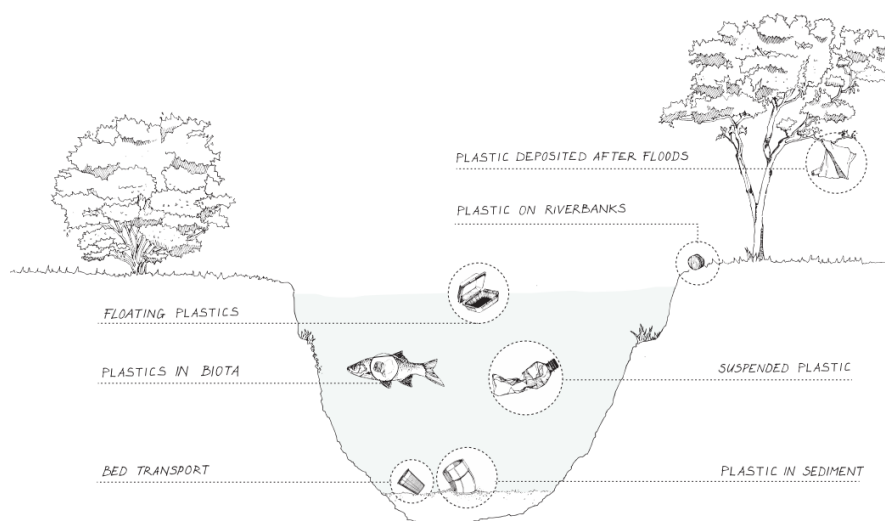

Figure 2: Plastic division in rivers (van Emmerik & Schwarz, 2019).

Most studies, in the field of riverine litter, focus on visible floating debris (van Emmerik & Schwarz, 2019). According to Morritt et al., (2014), submerged plastics can occur in large volumes and should also be taken into account when quantifying the plastic input from rivers into the seas.

1.2. Problem statement

As mentioned above, in the problem motivation, riverine litter, and especially submerged riverine litter remains understudied compared to marine-and floating litter. Based on plastic characteristics and turbulent river flow conditions, a considerable portion of the riverine litter can be transported underneath the water surface (van der Wal et al., 2015). Recent research shows that for uniform flow conditions, marginal buoyant plastics, foils specifically, might be uniformly distributed over the river depth (Zaat, 2020). This indicates that suspended plastics should be taken into account in order to quantify the total plastic transport via rivers.

Additionally, litter monitoring methods should be standardized. Until now there is no standard monitoring method for suspended riverine litter (González et al., 2016). Having a standard, widely applicable, monitoring method would enable comparing plastic transport in different river systems. Comparable information about plastic fluxes allows for indicating the most polluted rivers. Consequently, locations can be determined where mitigating measures are most necessary.

Current monitoring methods, regarding submerged riverine macroplastics, mainly involve the use of nets (van Emmerik & Schwarz, 2019). Different studies have been conducted using small nets, of usually 1 meter wide by 50 centimetres high. Additionally, fishing fykes and layered nets are operated (van Emmerik & Schwarz, 2019). The use of nets to sample suspended riverine macroplastics seems straightforward. However, there are some downsides regarding monitoring with nets that need to be considered.

First of all, the amount of material that is sampled using a net depends on the mesh size of the net (González et al., 2016). This induces a crucial choice on mesh size to be used in specific river basins, involving uncertainties and comparison difficulties regarding the amount of litter present. Moreover, the use of nets often depends on the availability of fixed structures, such as bridges crossing the river, to deploy the measuring equipment. The dependence on existing infrastructure limits the monitoring method to certain locations in river systems.
Furthermore, the use of nets implies stationary sampling. In large rivers, the spatial variability of submerged plastics over the cross-section is difficult to address using the net measuring technique. In the case of monitoring litter in large rivers, dynamic sampling from boats can be performed to cope with the variability of plastics in the river (González et al., 2016). To implement the dynamic measuring method correctly, the effect of the waves generated by the boat and motor propulsion should be taken into account. The generated waves can cause a disturbance in the vertical dispersion of particles, which may affect the monitored amount of riverine litter (González et al., 2016).

Lastly, nets usually only cover a part of the river depth. Deploying a net over the full depth is often not achievable because of large horizontal forces, caused by the river flow. In previous studies, small nets are used to avoid these large horizontal forces. The small nets can be deployed by two persons. For larger nets, cranes are needed, which makes this method labour intensive. The plastic litter that is monitored when using small nets is only a portion of the litter that is transported by the river. Since litter transport is not distributed evenly over the width of the river and likely also not over the depth, the plastic transport load can only be estimated (van Emmerik et al., 2018).

In summary, the applicability of the current monitoring methods for suspended macroplastics, as described above, is limited in several river basins. This makes the comparison of data on plastic fluxes problematic. To indicate the amount of plastic entering the seas via rivers and to optimize prevention and mitigation strategies, consistent measuring techniques are needed.

1.3. Research objectives

Based on the problem statement, research objectives were determined and formulated. The aim of this thesis is to develop and test a new technique for monitoring submerged riverine macroplastics. The new monitoring method has to meet the following objectives. Firstly, to enable comparing monitoring activities all over the world, the new method should be applicable in different river systems. Moreover, the second objective is to create a method that is independent of fixed structures for deployment. Furthermore, since current monitoring techniques often do not include the full depth of the river, this research focusses on monitoring litter over the entire river depth. The monitoring technique should fit use in data-scarce regions with high expected plastic concentrations. Finally, investment and deployment costs are taken into account.

Echo sounding is currently used for fish finding and seabed mapping. An echosounder transmits soundwaves and measures the difference in time between transmitted soundwaves and the received reflected signal. Signals reflect on sea bottoms and objects in the water column. To meet the mentioned criteria, echo sounding appears to be a suitable technique for monitoring suspended riverine litter. The possibilities and limits of the use of echo sounding are investigated. Moreover, the ability to identify plastics of different material types and sizes is studied. Being able to not only detect submerged plastic litter but also identify the items would allow for possible source identification and customized intervention measures.

1.4. Scope

To narrow the field of study, the scope of this research is defined. First of all, in this thesis, the focus is on monitoring submerged riverine plastics. Floating plastics or plastics at riverbanks are not taken into account. Furthermore, regarding the litter size, only macroplastics are considered in this research, which are objects larger than 2.5 centimetres (González et al., 2016). Moreover, this research focusses on testing and applying the use of echo sounding as a new technique for monitoring macroplastics in rivers. As echosounder, the Deeper CHIRP+, which is a low-cost off-the-shelf fishfinder of around 300 euros was used. This device was chosen due to its price, user-friendliness, and size.

The Deeper CHIRP+ was tested in a controlled environment, to investigate its abilities for plastic detection. Moreover, the performance of the sensor was tested in a natural environment. As case study areas, the Guadalete and Guadalquivir river basins in Southern Spain were used. Tests and monitoring were performed in the two river basins. The Guadalete and Guadalquivir river basins are known for their high plastic pollution rates, especially during periods of high river discharge.

1.5. Research question

Based on the research objectives and scope, the following research question and sub-questions are answered in this thesis.

Can echo sounding be used to detect and quantify macroplastics suspended in the water column, and if so, to what extent?

- ❖ *How does object detection with echo sounding work?*
- ❖ *What factors influence the detecting abilities of the echosounder?*
- ❖ *Can actual object size be determined by the sonar readings?*
- ❖ *Can a difference in material properties of litter be observed from sonar readings?*
- ❖ *To what extent can echo sounding be used to monitor the transport of suspended macroplastics in natural flows?*

1.6. Research method

In this section, the research method used to achieve the objectives is described. First of all, a general understanding of plastics, its types and characteristics was obtained by a literature review. Secondly, the presence of plastics in rivers, including the current state of research and monitoring techniques was considered. Specifically, the current monitoring techniques

for submerged macroplastics were analysed. Furthermore, a literature study on the principle of sonar and fish finding techniques was performed.

According to the literature review on both the sonar principle and riverine macroplastic monitoring, new monitoring-and test setups were developed in this study. To test the abilities of the sensor, the sensor was tested in a controlled, artificial environment and in a natural environment. To investigate the abilities of the sensor in an artificial environment, tests were executed in the Kerkpolderbad swimming pool, in Delft. The aim of the controlled tests in the artificial environment was to examine the relation between signal, object size, flow velocity, and depth. Furthermore, to investigate the abilities of the sensor for different types of plastics, in a natural environment, tests with plastic targets were performed in the Guadalete river basin, in Southern Spain. Lastly, the sensor was used for continuous monitoring of plastic litter in two natural rivers in Southern Spain. In the Guadalquivir river, the sensor was placed in front of two nets to compare the readings of the sensor with the litter caught in the nets. Moreover, monitoring took place in the Guadalete river for different tidal conditions and locations over the cross-section of the river.

After performing the experiments, as described above, the data were processed and analysed using MATLAB. With the use of the Image Processing Toolbox of MATLAB, the sonar signals are analysed on pixel level. Relations regarding signal size and intensity were investigated. In the end, the possibilities and limitations concerning the detection and identification of plastics with echo sounding were evaluated. The general steps taken during this research are presented in Figure 3.

Figure 3: Thesis research method overview.

1.7. Report outline

The remainder of this thesis is structured as follows. In Chapter 2, the theoretical background information relevant to this thesis is provided. In the first section, a summary of the relevant background information is given. The follow-up sections contain detailed information per subject. In section 2.2, the focus is on plastics in general and plastics in rivers. To get an understanding of the possibilities and limitations of echo sounding, the principles of sonar are described in section 2.3. The theory behind images and information about MATLAB, as image analysis software, is given in section 2.4.

In Chapter 3, an elaboration can be found on the methods used. The different methods are part of an iterative process, in which the method for testing the sensor was continuously adapted. The Methodology chapter is divided into two parts, the data collection part, and the data processing part. In the data collection part, section 3.1, information is provided regarding the study area and the used echosounder. Moreover, the three different methods for testing the abilities of the sensor are described. After the description of the process for the data collection, the steps taken for the data processing are explained in section 3.2. This includes the analysis of the collected data with the use of MATLAB.

The results and discussion chapter, Chapter 4, is structured based on the three different methods used for investigating the abilities of plastic detection with echo sounding. For each method, the results are presented first, whereafter the results are discussed. To begin with, the results and discussion concerning the controlled tests in the artificial environment are provided in section 4.1. In section 4.2, the findings regarding the semi-controlled tests in the natural environment are shown and described. Finally, the outcome of the monitoring activities is given in section 4.3. In Chapter 5, an overall discussion of the three different experiments and results is provided. In Chapter 6, the conclusions and recommendations regarding the research of this thesis are given.

2.
Theoretical background

In this chapter background information, regarding this thesis, is provided. First, a summary of the necessary background information is given. More detailed information is presented in the remaining sections. In section 2.2, the different characteristics, properties and uses of plastics are described. Thereafter, an insight into European riverine litter is given. Furthermore, an overview of the presently used monitoring methods and their application is presented. In section 2.3 the principle of sonar, including the fishfinding ability is explained. Lastly, in section 2.4, information important for the sonar data processing, using image analysis, is provided.

2.1. Summary

Monitoring techniques regarding suspended macroplastics remain limited. Current monitoring methods, which make use of nets, have several disadvantages when it comes to estimating river fluxes. To correctly determine riverine litter transport, the suspended litter should be taken into account. Sonar could potentially be used for monitoring suspended litter.

The sonar principle works by transmitting soundwaves into the water, which reflect on objects like fish, vegetation, and soil. The reflectance time and the strength of the returning pulse are measured (Deeper, 2019). The time it takes for a pulse to return indicates the position of objects in the water column. The strength of the returning pulse is related to the robustness of the material or bottom. The transmitted sound waves travel in the shape of a cone. The size of the cone depends on the frequency with which the signal is emitted (Deeper, 2019). In general, the higher the frequency, the smaller the cone angle.

There are different types of sonar. In this research, a single beam echosounder with CHIRP technology is used. A CHIRP sonar emits a continuous flow of varying frequencies, while a traditional sonar sends out a single frequency pulse at a time. Emitting pulses with different frequencies, ranging from low to high, results in clearer sonar readings of higher resolution and improved target separation compared to traditional sonars.

Sonar readings are generated by the backscatter intensity of transmitted pulses. The signals presented on the display are a result of a 2D scan over the depth. The horizontal axis on the display indicates time, the depth is presented on the vertical axis. The strength of the returning signal is indicated by the colour displayed on the screen. Water does not reflect sound at all, in contrast, air has a high sound wave reflectivity. Surface clutter causes blind zones at the top of the water column, for which the sensor is not able to detect any objects. Fish are displayed as arches on the sonar readings.

For this research, the Deeper CHIRP+ was used, which is a commercial fishfinder with CHIRP technology. The Deeper CHIRP+ allows for scanning with three different beamwidths, corresponding to different frequency ranges. Raw sonar data cannot be exported, therefore, the sonar images, obtained during this study, were analysed in MATLAB. The sonar images are presented in an RGB colour scale. Pixels presenting the sonar signal are separated from the background pixels using K-Means clustering.

2.2. Plastics

In this section, information about plastic types, composition, and use is provided. Moreover, insight is given in research regarding litter in European rivers, litter size fraction and litter composition. Furthermore, current monitoring techniques, regarding both floating and submerged litter, for riverine macroplastics are described.

2.2.1. Plastic definition, composition and types

The term plastic is derived from the Latin "plasticus" which was used to describe something able to be moulded or fit for moulding (PlasticsEurope, 2018). Today, the term plastic is used to describe a large family of very different materials with different characteristics, properties and uses (PlasticsEurope, 2018). Since the term plastic covers a various range of items, a distinction in categories is made based on different plastic characteristics and properties. Table 1 gives an overview of the different categories of plastics and their use.

Table 1: Plastic categories and use (van Emmerik & Schwarz, 2019; PlasticsEurope 2019).

Name	Abbreviation	Use
Polypropylene	PP	Food packaging
Polyethene, low density/Polyethylene, linear low density	PE-LD/PE-LLD	Reusable bags, trays, and containers
Polyvinyl chloride	PVC	Construction products
Polyethene terephthalate	PET	Bottles
Polyethene, high density/Polyethylene, medium density	PE-HD/PE-MD	Toys, milk bottles, shampoo bottles, pipes
Polyurethane	PUR	Building insulation, matrasses
Polystyrene/Polystyrene, expandable	PS/EPS	Plastic cups

It can be noticed in the table above that the plastics currently used have different material properties, which makes studying plastic litter challenging.

2.2.2. European Riverine litter

As stated by the European Commission, between 150 000 and 500 000 tonnes of plastics enter the oceans each year by European rivers. Related to the estimated total plastic transport into the oceans across the world this only represents a small portion. However, the plastic waste, transported by European rivers, end up in particularly vulnerable marine areas, such as the Mediterranean Sea and parts of the Arctic Ocean (European Commission, 2018).

European riverine litter has been subject to several studies. According to a recent study on monitoring macroplastics, only 3 out of 20 studies focussed on suspended plastics (van Emmerik & Schwarz, 2019). In the next section, more information about the currently used monitoring methods is given.

According to González et al., 2016, litter can be divided into the following categories based on size:
Macro (> 25 mm)
Meso   (5-25 mm)
Micro (<5 mm)

This research focuses on the category of macro litter, which means objects of 2.5 centimetres or larger.

Based on a literature study regarding European riverine litter, information about litter items present in European rivers was obtained. Looking at studies concerning suspended plastics, the study of Hohenblum et al., 2015, where plastics suspended in the water column were monitored, observed a majority of polyethene and polypropylene plastics. According to Table 1, this corresponds to reusable bags, trays, containers and food packaging. Another study of interest, using fishing fykes for monitoring river bed litter in the Thames (Morritt et al., (2014)) observed a presence of mainly food wrappers, food containers, sanitary towels, plastic bags and plastic cups/cutlery. The insight in suspended litter present in European riverine environments enabled determining the requirements for the use of sonar for plastic detection for this research.

2.2.3. Current monitoring methods for riverine macroplastics

Monitoring riverine macro litter is executed in various manners. As mentioned before, in general, a distinction is made between plastics in the water body and on the river bank. For the purpose of this research, the monitoring of riverbank litter is not taken into account. When it comes to litter in the river water body, there is a division made based on the presence of plastics in the vertical river profile. At the water surface, there are floating litter items present, in the water column litter items in suspension, and at the river bottom, plastics can be transported as bed load.

Water surface

Litter present at the water surface, or floating litter, is monitored in several studies across Europe. According to (van Emmerik & Schwarz, 2019), the following monitoring methods, regarding floating litter, are currently used.
- Passive sampling
- Net sampling
- Visual counting

For passive sampling, existing infrastructure is used to collect litter. This method is applied in the Seine river by Gasperi et al., (2014). Floating debris retention booms were used to analyse litter present at the water surface, illustrated in Figure 4. The advantage of passive sampling is that there is no need for investing in monitoring installations. However, flexible deployment is not feasible and therefore, this method is not always useful for specific research (van Emmerik & Schwarz, 2019).

Figure 4: Surface litter collecting using an existing floating boom in the Seine (Gasperi et al., 2014).

When looking at the net sampling method, small nets are deployed from bridges to collect litter samples. According to van Emmerik & Schwarz (2019), often nets of 1 m wide and 0.5 m tall are used and can be deployed by one or two persons. In this way, litter from the water surface and the upper layer of the water column can be collected. The use of these nets allows for sampling at different locations over the cross-section of the river. Also, the focus can be on specific targets by adjusting the mesh size of the net. The disadvantage is that the monitoring method depends on the availability of fixed structures, such as bridges. Moreover, the nets can only be used under limited flow velocity conditions, otherwise deployment becomes problematic due to significant horizontal drag (van Emmerik & Schwarz, 2019).

Another widely applied method to quantify floating litter is visual counting from bridges. The visual counting method is executed by observers, standing on a bridge, counting the passing litter items for a certain time. This monitoring method is executed on more than 40 rivers as part of the European RIMMEL network (González-Fernández). The advantage of this method is that the plastic distribution over the river width can be investigated. However, to cover the total river width, for large rivers, many observers are needed, which makes this method labour intensive. Additionally, uncertainties regarding observer bias and plastic size (turbidity and bridge height) have to be taken into account. Recently, the use of cameras, Unmanned Aerial Vehicles, and satellites to count floating litter are under development (van Emmerik & Schwarz, 2019).

Water column

The part of the litter that is present in the water column, also known as suspended litter, is, as mentioned in the introduction, currently monitored with the use of nets. As described above, at the water surface monitoring, small nets are used to monitor the submerged plastics in the upper layer of the water column. Often, when using these small nets, also floating litter is collected. This makes determining quantities of submerged litter difficult. In the study of van der Wal et al., (2015) small nets were used which were deployed 20 to 70 cm below the water surface to collect suspended litter. Moreover, net sampling with a three-layered net, deployed from a crane was executed in the Danube river by Lechner et al., 2014; Hohenblum et al., 2015; Liedermann et al., 2018, shown in Figure 5.

Figure 5: Three-layered net for suspended litter collection, deployed from a crane (Hohenblum et al., 2015).

As previously mentioned, the choice of the mesh size of the net is crucial. On the one hand, the ability to change the mesh size allows for broader applications. On the other hand, monitoring activities are challenging to compare when different mesh sizes are used. Furthermore, the use of nets depends on the availability of fixed structures such as bridges to deploy the nets. The use of cranes is expensive and labour-intensive. Additionally, monitoring submerged plastics using nets provides stationary sampling. The nets cannot easily be deployed over the full river width, which makes investigating the litter transport over the cross-section complex. Finally, nets cover usually only a portion of the water column. Horizontal forces due to the flow velocity of the water induce difficulties using a net over the full river depth.

River bottom

Litter transport at the bottom of the river, or so-called river bed litter transport, was investigated by Morritt et al., (2014). Specifically, the river bed transport in the upper Thames was studied using eel fykes attached to the river bottom. A sample of trash caught in a fyke is shown in Figure 6.

Figure 6: Litter present at the river bottom trapped in eel fyke (Morritt et al., 2014).

Furthermore, plastics present at the river bottom are studied by taking sediment samples. Sediment samples were taken during the study of Tuscan rivers in Italy by Cannas, Fastelli, Guerranti, & Renzi, 2017. However, most items found were in the categories of microplastics.

According to the above-provided information about the current monitoring techniques, monitoring suspended macroplastics remains limited, especially compared to floating litter. The current methods, which make use of nets, have several disadvantages when it comes to estimating river fluxes. According to van der Wal et al., (2015), litter characteristics and turbulent flow suggest that a major fraction of the litter can be transported in the water column, below the surface. To correctly determine riverine litter transport, the suspended litter should be taken into account.

2.3. Sonar

As explained in the previous section, there is a need for a method to monitor suspended plastics: this is where sonar comes in. In this section, the principle of sonar is explained, including the different types of sonar. For this study, in particular, the capabilities of detecting transported litter in deeper layers of the water column is of interest. Hence, attention to the fish finding capacity of sonar is given. Besides, detailed information about the used sensor, the Deeper CHIRP+ is provided.

2.3.1. The principle of sonar

Sonar stands for Sound Navigation Ranging. The sonar principle works with transmitting soundwaves into the water, which reflect on objects like fish, vegetation, and soil, illustrated in Figure 7. The reflectance time and the strength of the returning pulse are measured (Deeper, 2019). The time it takes for a pulse to return indicates the position of the object in the water column. The strength of the returning pulse is related to the robustness of the material or bottom.

The use of echo ranging to detect and locate underwater objects originates in the 20th century (Ainslie, n.d.). The development of this technique was induced by the sinking of the RMS Titanic in 1912 and the First World War (Ainslie, n.d.). For a long time already, the principle of echo ranging is used by for eg. dolphins and whales to detect obstacles (Ainslie, n.d.). Currently, sonar is used for navigation and object detection purposes, including fish finding.
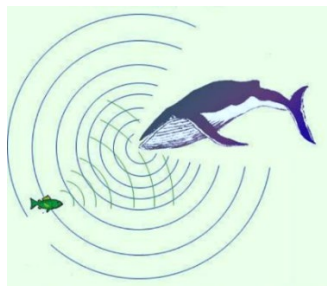

Figure 7: Example Sonar principle whale (Yngstr's Weblog, 2008).

Sound waves

As described above, the principle of sonar works by transmitting a sound wave and receiving the reflected signal. The speed of sound waves differs per substance. Assuming room temperature (20-25 degrees), in air, the speed of sound is 337 m/s. In water, the wave velocity is higher and about 1490 m/s for freshwater and 1533 m/s for saltwater (Ainslie, n.d.). This high soundwave velocity in water is useful for scanning the seabed with the use of sonar (Brown, 2019). The velocity of the sound wave determines the propagation of the sound in water. In general, the soundwave velocity depends on water density and compressibility. The water density and compressibility can be described by three variables, namely, temperature, salinity, and pressure. The soundwave velocity in seawater increases with increasing temperature, salinity, and pressure. According to the Mackenzie equation (1981), formula (1), the potential change in the soundwave velocity is determined and presented in Table 2. The calculated differences are based on the range of validity of the Mackenzie formula, which is; temperature 2 to 30 °C, salinity 25 to 40 parts per thousand, and depth 0 to 8000 m.

$$c(D,S,T) = 1448.96 + 4.591T - 5.304*10^{-2}T^2 + 2.374*10^{-4}T^3 \\ + 1.340(S-35) + 1.630*10^{-2}D + 1.675*10^{-7}D^2 - 1.025 \\ *10^{-2}T(S-35) - 7.139*10^{-13}TD^3 \qquad (1)$$

With T = temperature in degrees Celsius, S = salinity in parts per thousand, and D = depth in meters.

Table 2: The potential difference in soundwave velocity caused by the factors temperature, salinity and depth, based on the Mackenzie formula.

Parameter	Potential difference in soundwave velocity (m/s)
Temperature	86
Salinity	17
Depth	132

Another factor that influences the sonar readings is turbidity (Christ & Wernli, 2014). Turbidity is a measure for the content of suspended solids in water and can cause scattering. Scattering regarding sound waves can be described as molecules in the water blocking the sound wave (Christ & Wernli, 2014).

Cone-shaped sound waves

The transmitted sound waves travel in the shape of a cone, illustrated in Figure 8. The size of the cone depends on the frequency with which the signal is emitted (Deeper, 2019). In general, the higher the frequency, the smaller the cone angle. The spherical shape of the sound wave is caused by the outward propagation of the pressure-based disturbance. Moreover, a sound wave is generated due to the expansion or contraction of a source at a given frequency. The motion of the source results in an increase in the density of the surrounding fluid (Ainslie, n.d.). Due to the increase in density, an increase in pressure is also caused, resulting in a cone-shaped wave.
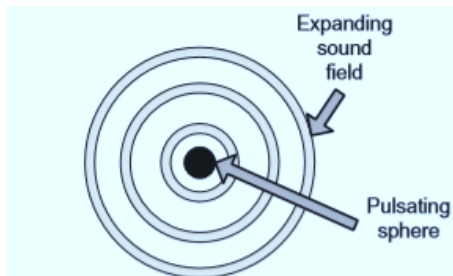

Figure 8: Top view cone shape sound wave (Christ & Wernli, 2014).

Different types of sonar

There are different types of sonars. A general division is made between active and passive sonar. An active sonar consists of a transmitter and a receiver (Ainslie, n.d.). This system

makes use of locating by echoes. The time difference between the outgoing wave and the incoming echo of that wave is measured and translated to distance. Radar and dolphins use active sonar to locate objects. Passive sonar has a receiver but no transmitter. The signal that is detected is the sound emitted by the target (Ainslie, n.d.). In this research, the active sonar type is used. When looking at active sonars, there are three different types, the single beam (A), side-scan (B) and multibeam sonar (C), presented in Figure 9.
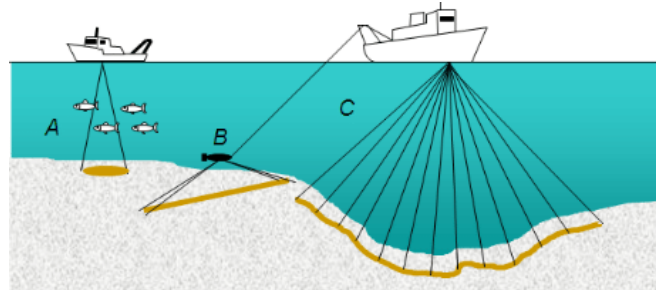

Figure 9: Schematic representation of the three main sonar types (Lurton & Lamarche, 2015).

The single beam sonar, as the name already indicates, scans with a single beam at the time. The beamwidth determines the area which can be scanned. This is the oldest and lowest-priced type of echosounder. It has a lower spatial resolution compared to the other two types. The second type, the side-scan sonar, can quickly scan a large area and provides a detailed image of objects on the bottom. Lastly, the multibeam echosounder scans with multiple beams at the same time and can give a 3D image of the water column and sea/river bed. Multibeam echosounders are most expensive compared to single beam and side scan sonars.

For this research, a single beam sonar was used. The traditional single beam echosounder emits sound waves with one frequency at the time. There are also single beam sonars that make use of the CHIRP technology. The CHIRP (Compressed High Intensity Radiated Pulse) technology differs from traditional sonars in the way frequencies are emitted. A CHIRP sonar emits a continuous flow of frequencies, while a traditional sonar sends out a single frequency pulse at a time (Deeper, 2019). Emitting pulses with different frequencies, ranging from low to high, results in clearer sonar readings of higher resolution and enables improved target separation compared to traditional sonars (Deeper, 2019). Figure 10 shows the general principle of CHIRP technology.
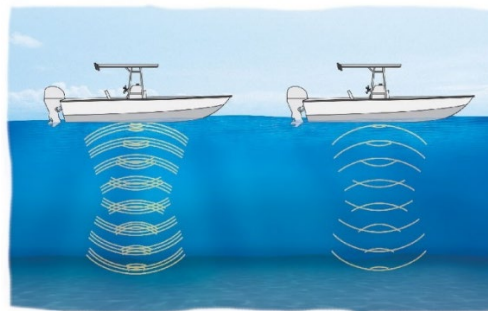

Figure 10: Illustration of CHIRP vs traditional sonar transmitted sound waves (Hendricks, 2018).

In more detail, the ability of an echosounder to identify and separate targets depends on the pulse length (Christ & Wernli, 2014). The transmitted pulse length has to be relatively long to detect targets in a wide range (Christ & Wernli, 2014). However, a long pulse length results in a lower range resolution, and therefore less accurate target separation, indicated in the formula below (Christ & Wernli, 2014).

$$S = \frac{c_0 * \tau}{2} \tag{2}$$

In which S is the range resolution, τ is bandwidth, c_0 is the velocity of sound. The usual pulse duration or bandwidth for a traditional sonar is 50 µs.

To overcome the above-mentioned limitation, CHIRP technology can be used. As displayed in Figure 11, when CHIRP is used, the transmitted pulse consists of a range of frequencies, instead of the single frequency of traditional sonar technology. The different transmitted frequencies are matched to the signal returns by 'pattern-matching' (Christ & Wernli, 2014). The range resolution of the CHIRP based sensor depends on the bandwidth of the pulse. A typical bandwidth for the CHIRP sensor is 100 kHz, this results in an improvement in range resolution by a factor 5, compared to the traditional sonar.
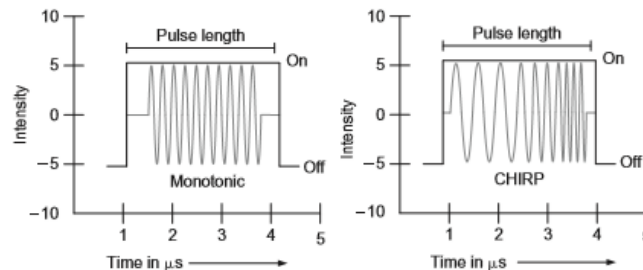

Figure 11: Pulse frequencies for a traditional vs CHIRP sonar (Christ & Wernli, 2014).

Additionally, the functioning of a traditional sonar, compared with the CHIRP technology, for separating targets is illustrated in Figure 12.
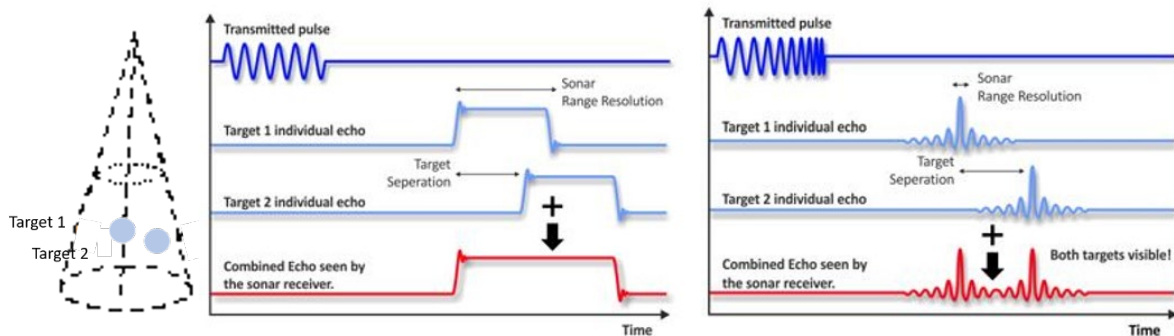

Figure 12: Target separation for traditional sonar (left) vs CHIRP sonar (right) (Deeper, 2019).

Sonar images

Many echo sounding appliances translate sonar scans into images. A sonar image can be categorized as having a lower resolution compared to an optical image as a consequence of the compilation of the image from the ultrasonic signal (Christ & Wernli, 2014). Sonar images are generated by the backscatter intensity of transmitted pulses.

The signal emitted by the sonar diverges over the depth. The sonar signals presented on a display are a result of a 2D horizontal scan over the depth. The spherical horizontal scanning plane at a certain depth is converted to a single point at the display (Hedquist, 2016). Emitting a burst of pulses results in several points over the depth. This results in a vertical profile of the single points at a certain moment in time, see Figure 13. When displaying continuously, the horizontal axis on the display indicates time, the depth is presented on the vertical axis. Moreover, the sonar readings are presented on the display using a specific colour palette. The colours indicate the signal strength. An example illustrating the readings on a display is provided in Figure 13.
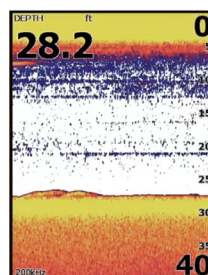

Figure 13: Example of single beam sonar reading (Panbo, 2019; Hedquist, 2016).

Reflectance properties objects

In general, objects with rough surfaces can easier be detected using sonar than objects with smooth surfaces because sound waves are well reflected in many directions by rough objects (Christ & Wernli, 2014). Smooth objects also reflect sound well but in fewer directions or one direction (Christ & Wernli, 2014). When sound waves are reflected in many directions, the probability for the sonar to detect the returning signal, and therefore, locate objects is higher than when sound is reflected in fewer directions. Table 3 shows the reflectivity of different substances that can be present in aquatic environments.

Besides measuring the time between transmitting a pulse and the returning pulse, sonars also measure the strength of the returning signal. The strength of the returning signal indicates the density of objects or the sea/river bottom and is indicated by the displayed colour. Objects of high density (hard objects) return stronger signals than low density (soft) objects. Water does not reflect sound at all (Christ & Wernli, 2014). The reflectance strength of the sonar signal is also influenced by density differences. The difference in density between (sea)water and air is approximately a factor ten, resulting in a high reflectivity of air(bubbles) present in the water.

Table 3: The echo sounding reflectivity on different substances (Christ & Wernli, 2014).

Substance	Relative reflectivity
Water	None
Mud	Low
Sand	Medium
Rock	High
Air/air-filled	Very high

Another factor that can influence the detection of objects is surface clutter, indicated in the top layer in Figure 13. Surface clutter is caused by the water surface, which reflects some of the emitted sonar signals directly. The signals reflected by the water surface are too fast for the sonar to process. This is due to the short distance between the sensor and the water surface. There are several reasons for the signal to reflect on the water surface. The most likely reason is the presence of waves, air bubbles, current, or algae (Deeper, 2019). When there is significant surface clutter, a blind zone is formed. In the blind zone, which is a layer of a certain depth from the water surface, no objects can be detected. All sonars have blind zones, the size of the blind zone can, however, be limited by using a high scanning frequency. High scanning frequencies relate to small soundwave cones, resulting in scanning smaller areas. Using a sonar with CHIRP technology reduces the blind zone significantly (Deeper, 2019).

2.3.2. Sonar fish finding application

Sonar is used for different purposes, with fish finding being one of them. In general, a conventional fishfinder is a single beam sonar, which only scans in the vertical direction. Other types of sonar, such as multi-beam and side-scan sonar, could in principle also be used for fish finding, however, the equipment is more expensive. Conventional fishfinders can be bought in the range of 100 euros.

Fishfinders, or single beam sonars, emit a pulse of one frequency at a time. A cone of a certain radius is formed for which the area is scanned. For some devices, the scanning frequency, and thereby the cone radius can be selected. Frequencies usually range from approximately 100 kHz – 290 kHz for traditional fishfinders and up to 675 kHz for a fishfinder with CHIRP technology (Deeper, 2019).

The displayed signals on fishfinders are a result of a 2D horizontal scan over the depth. Since the 2D spherical plane is transformed to one point, no indication of where the fish is present in the scanned horizontal plane can be obtained. Only information about the position of fish in the depth of the water column can be collected.

There is often an algorithm included in fishfinders, where fish icons can be displayed to indicate fish. The accuracy of using these fish icons is however as yet undetermined. It is therefore recommended to switch the icons off if you want to obtain more accurate readings on numbers of fish and fish size (Deeper, 2019). In general, fish reflect sound waves well due to their gas-filled bladders. Fish passing the sensor are displayed as arches. This is explained by when a fish enters the scanning cone at the side, there is a larger distance between the fish and the sensor than when the fish passes the cone in the centre (University of Rhode Island, 2019). The same holds for when the fish swims out of the cone again, leaving an arch on the display. The arches can vary in size and are only present when the fish moves. A full arch is displayed when a fish swims through the entire cone. Half arches can indicate fish that only swim through a part of the scanning cone. The way fish is presented on the sonar display is illustrated in Figure 14.
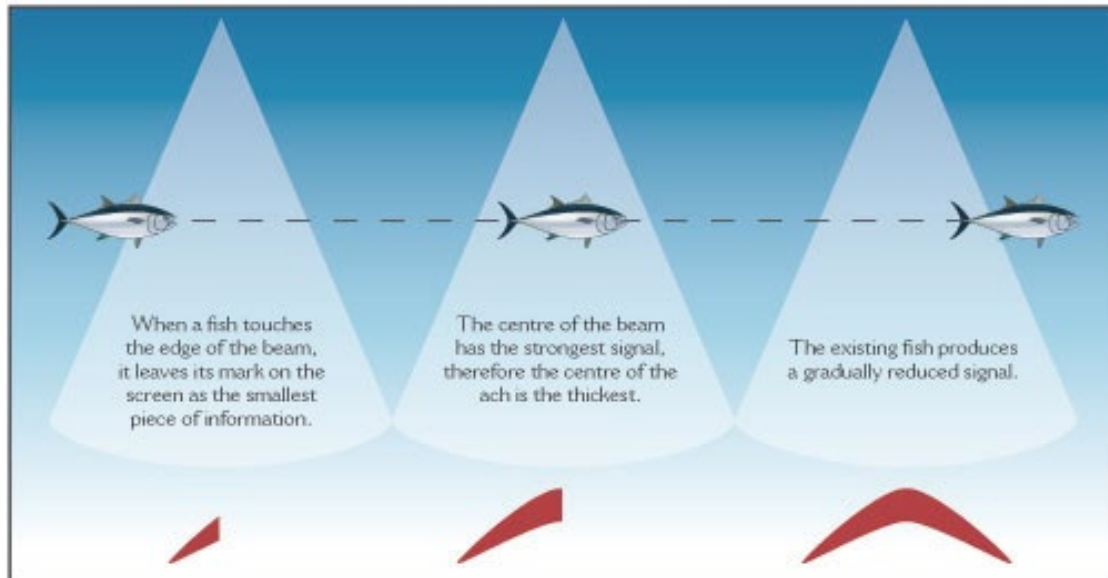

Figure 14: The development of the arch shape generated by fish on sonar readings (Outdoor Nirvana, 2019).

A mistake that is easily made when looking at the sonar data on the display is to count more fish then there are in reality (Deeper, 2019). This can be because when a fish is stationary under the sensor, and the sonar is immobile, the fish will be constantly displayed. As mentioned above, the horizontal axis of the display represents time, not distance.

If an indication of fish size is preferred, one should look at the thickness of the signal, rather than the length of the signal (Deeper, 2019). An example image of fish detected by the Deeper CHIRP+ fishfinder is presented in Figure 15. More information about the Deeper CHIRP+, which is used for this research, is provided below.
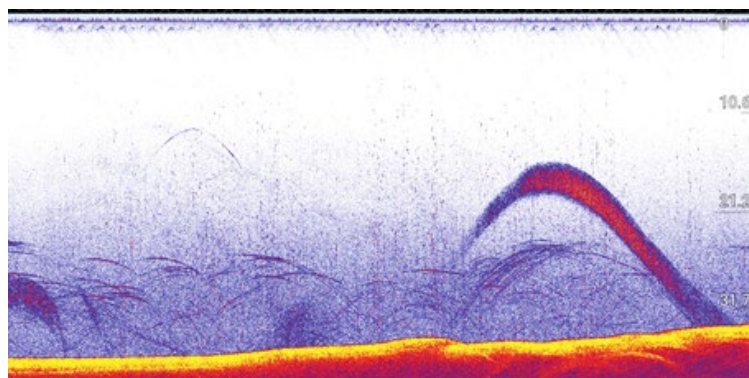

Figure 15: Example of fish on a sonar display (Deeper, 2019).

2.4. Signal image analysis (software)

Since raw sonar data, obtained with the Deeper CHIRP+, cannot be exported, images (screenshots) from the signals were analysed. For analysing these sonar images, MATLAB, version R2018b was used. The 'Image Processing Toolbox' package was installed to perform image processing, visualization, and analysis. Using MATLAB, the number of pixels per sonar signal is calculated and pixel intensity values are derived. An example image of a sonar signal to be processed in MATLAB is provided in Figure 16.
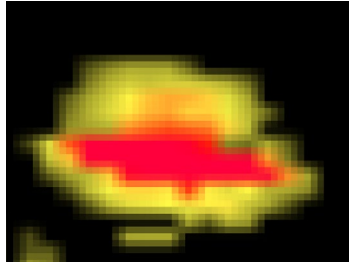

Figure 16: Sonar image (from a balloon) obtained with the Deeper CHIRP+, before processing in MATLAB.

To calculate the number of pixels of the sonar signal reflectance, and thereby the dimensions of the sonar signal (in pixels), the sonar signal is separated from the background pixels of the obtained image. For this separation, image segmentation is used. Image segmentation, in general, involves splitting an image into different regions of pixels (Chauhan, 2019). Splitting the image results in an image divided into different segments. The advantage of segmenting an image is that processing can be executed per segment instead of the entire image (Chauhan, 2019).

Image segmentation can be performed with various techniques. In this thesis, K-Means clustering is used for image segmentation. K-Means clustering is a relatively simple and popular image segmentation tool (Garbade, 2018). The K-Means clustering algorithm is an unsupervised algorithm that segments the area of interest from the background by defining clusters of similar data (Chauhan, 2019). When clusters of similar data are formed, centroids of each cluster are determined. The K-Means clustering algorithm is based on the formula provided below (Chauhan, 2019). In words, the sum of the squared distances between the data points and the centroid is minimized.

$$ J = \sum_{j=1}^{k} \sum_{i=1}^{n} \left\| x_i^{(j)} - c_j \right\|^2 \tag{3} $$

In which J is the objective function, k the number of clusters and n the number of cases. The absolute function (between brackets) is called the distance function in which x is case i and c the centroid for cluster j.

K-Means clustering is a built-in algorithm in the Image Processing Toolbox of MATLAB. The corresponding MATLAB script is provided in Appendix D). Although the surface area of the sonar signals is not smooth, see Figure 16, no threshold was needed for separating the sonar signal from the background of the image.

The screenshots taken from the sonar signals are RGB images. RGB stands for red, green, blue and belongs to the RGB colour model, shown in Figure 17. The RGB colour model is an additive colour model, in which model light is used to display colours (Educba, 2019). Digital displays such as TVs, computer displays and digital cameras use this colour model to display colours. In general, a colour model is used to create an array of colours using primary colours. In the RGB colour model, the primary colours are red, green and blue. The colour black is displayed if the least intensity values of the three colours are added. When red, green and blue are superimposed with the full intensity of light, the colour white is formed. In order to create an array of different colours, primary colours with different intensities are added.

Figure 17: RGB colour model (Wikimedia Commons, 2019).

The range of colour intensities depends on the datatype class of the RGB image array. When using MATLAB, the RGB image array can be of the class 'double', 'unit8' and 'unit16'. The 'double' datatype class represents colour components with values between 0 and 1. If an RGB image is of the 'unit8' class, the colour component value ranges between 0 and 255. For the 'unit16' class, values differ between 0 and 65535 (Hritik, 2019). In this research, images of the 'unit8' datatype class were used. The primary colours, in this case, are expressed in 256 shades.

Additionally, an RGB image is structured as displayed in Figure 18. The three primary colour images are stacked on top of each other and displayed as a full colour image. In MATLAB, an RGB image is presented as an array of the form M*N*3. Each pixel in the image consists of three values for the red, green and blue colour. In other words, the combination of red, green and blue intensities determines the pixel colour. The colour planes are M*N arrays and together form the image in M*N*3 format. As an example, the pixel value of the upper left pixel (Pixel$_A$) is (255,0,255) which consists of a pixel value of 255 in the red colour plane, 0 in the green colour plane and 255 in the blue plane.
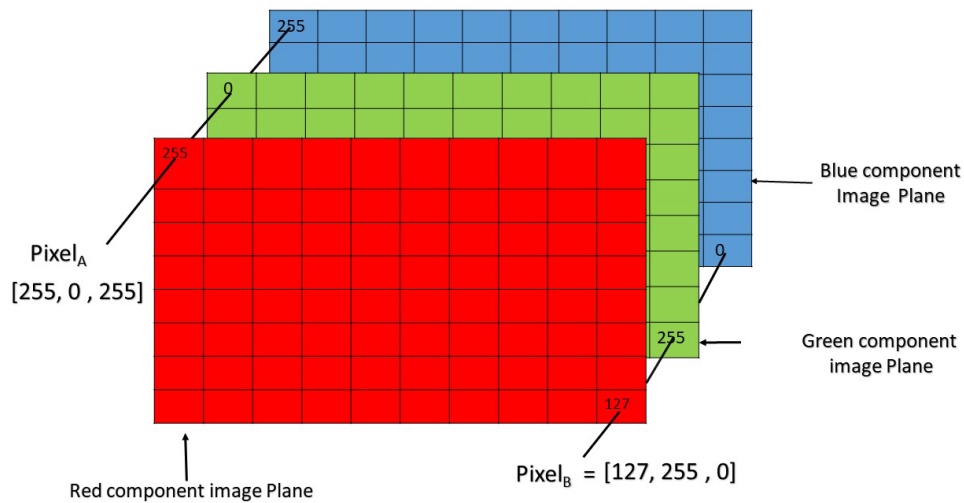

Figure 18: Example RGB pixel values of an image (Hritik, 2019).

Figure 19 presents the split R-G-B channels for the example sonar reading. Combining these three images lead to the original image as displayed in Figure 16.
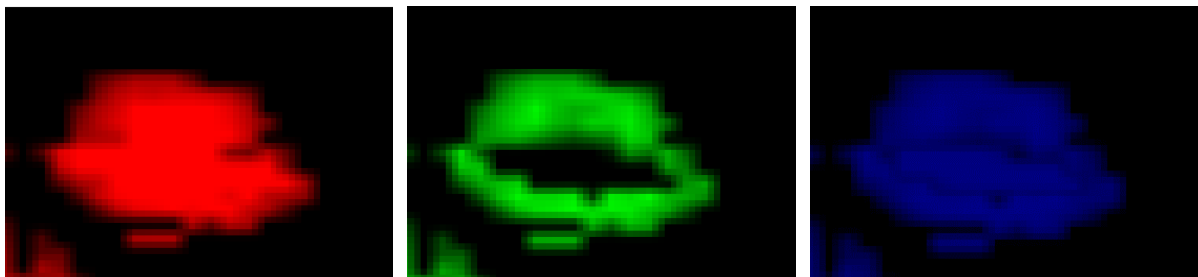

Figure 19: Split R-G-B channels in MATLAB for an example sonar reading (balloon) obtained with the Deeper CHIRP+.

The images from the sonar readings are analyzed based on the principles described above. Information on how this is executed is provided in the data processing section (3.2) of the methodology chapter.

To analyse the obtained data during this research, the calculated sonar signal dimensions are presented using boxplots. For the boxplot generation and the determination of outliers, the Interquartile Range (IQR) was used. The IQR is determined using the 25th (Q1) and 75th (Q3) percentiles of the data (IQR = Q3 – Q1). The upper and lower bound of the data are determined using a factor k. In this research, k is taken as 1.5. The upper and lower bound are determined using Q3 + (1.5*IQR) and Q1 – (1.5*IQR), respectively and indicated by whiskers. Data points that are outside the range determined with the lower and upper bound are presented as dots and defined as outliers. This is illustrated in Figure 20.
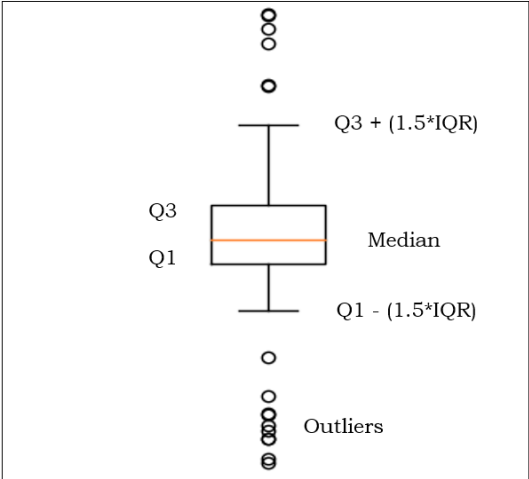

Figure 20: Used boxplots explanation based on the interquartile range (IQR).

3.

Methodology

The main goal of this research is to investigate the ability to detect submerged macroplastics using echo sounding. The applied approach for reaching this goal is described in this chapter. This chapter consists of two main parts, the data collection and the data processing part. The data collection was scaled up from a controlled small scale, in an artificial and riverine environment, to data collection in a naturally flowing river, illustrated in Figure 21. Several experiments, at different locations, were executed to investigate the possibilities and limitations of the use of echo sounding for plastic detection. The experiments were performed in three different manners, including, controlled tests in an artificial environment (swimming pool), semi-controlled tests with targets in a natural environment (river), and litter monitoring in natural flowing rivers. Detailed information about the aim and execution of the three methods is provided in section 3.1.
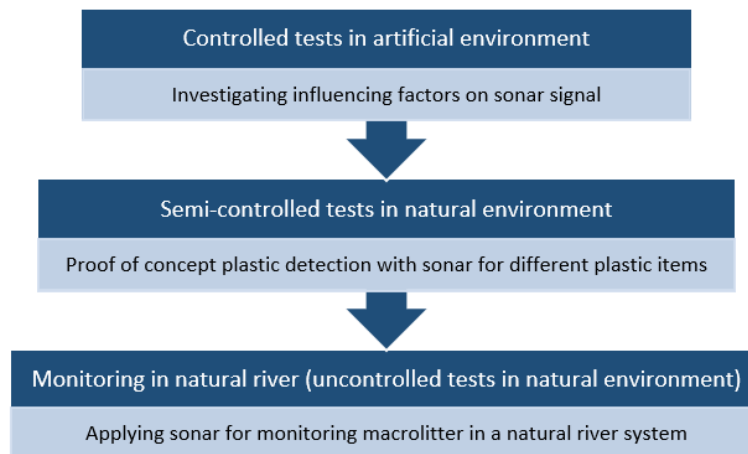

Figure 21: Schematic overview of the methods and aims concerning the performed tests for investigating the plastic detection abilities of the echosounder.

After the data collection phase, the sonar data were processed using MATLAB as an image analysis program. Since exporting raw sonar data was not feasible, screenshots of the sonar signals were taken to analyse. The specifics regarding the data processing are described in section 3.2.

3.1. Data collection

In this section, the study areas and their characteristics are described. Thenceforth, the procedures regarding data collection, for the three different methods used, are explained. The main aim of the executed methods is also stated.

3.1.1. Specifications echosounder used

As described in the Chapter 'Theoretical background', there are different types of echosounders. For the purpose of this research, a single beam echosounder with CHIRP technology was used. The main motivation for this choice is the affordable but advanced features of this type of echosounder. During preliminary tests, different echosounders were tested. Taking costs, user-friendliness, and size into account, the Deeper CHIRP+ was chosen.

Specifications Deeper CHIRP+

In this study, the Deeper Smart Sonar CHIRP+, which is a commercial fishfinder of approximately 300 euros, was used. This is a floating, castable, GPS and Wi-Fi enabled fishfinder, using CHIRP technology. The Deeper CHIRP+ enables scanning with three different beamwidths, with different frequency domains, which allows accurate target determination and separation (Deeper, 2019). Figure 22 shows the three beams which can be used for scanning the aquatic area with the Deeper CHIRP+. The wide beam is used for scanning larger areas with the least precision. The medium beam can be used in more shallow waters. The narrow beam is most precise. The different beamwidths correspond with different scanning frequency ranges, which are presented in Table 4. In shallow water, of less than 1.8 meters depth, only the narrow beam can be used for scanning, due to the presence of strong surface clutter for the wider beams. Independent of the beamwidth, 15 pulses per second are transmitted by the device.

As mentioned before, blind zones, related to surface clutter, cause sonar interference on the water surface. In the blind zone, the sonar is not able to detect objects such as fish. The surface clutter and so the blind zone depends on the beam angle and frequency used. There is small surface clutter when scanning with a high frequency, and so less depth is needed to operate the device. The blind zones per beam angle, for the Deeper CHIRP+, are shown in Table 4.
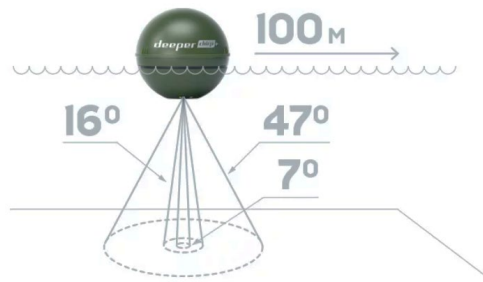

Figure 22: Available beamwidths of the Deeper CHIRP+ (Deeper, 2019).

Table 4: Specifications of the different beamwidths for the Deeper CHIRP+ (Deeper, 2019).

Beam	Cone angle (degrees)	Ultrasound frequency range (kHz)	Target separation (cm)	Blind zone (m)
Narrow	7	635 - 715	1	0.15
Medium	16	270 - 310	2.4	0.6
Wide	47	90 - 115	2.4	0.8

Sonar type*:*
3 Frequency CHIRP
Depth range:
15 cm – 100 m
Wi-Fi range:
100 m
GNSS (Global positioning systems supported):
GPS, GLONASS, Galileo, BeiDou, QZSS

The Deeper CHIRP+ operates with the Deeper Smart Sonar application (app), which can be installed on a telephone or tablet. In the app, the different settings, such as the beamwidth and sensitivity can be selected. By adjusting the sensitivity, clutter can be removed from the sonar readings. Furthermore, the colour palette in which the sonar readings are displayed can be selected. In this research, the Classic colour mode is used. Besides the sonar readings, information about the water depth and temperature are provided in the app. The sonar scan data can be saved and uploaded to Lakebook. Lakebook is an online platform where data of the scanning activities can be stored and viewed. From Lakebook, only raw bathymetry data can be exported as CSV format. Exporting raw data on signal strength and intensity is, currently, not possible.

3.1.2. Study area

The controlled tests were executed in the water laboratory at the TU Delft and the swimming pool Kerkpolder, in Delft, The Netherlands, in the period July – December 2019. First tests were performed in the Hydraulic Engineering Laboratory of the Civil Engineering faculty at the TU Delft. The sonar signal, however, reflected strongly on the sides and bottom of the available tanks and flumes, inducing noise in the sonar readings. Also, the depth of the tanks and flumes was not sufficient to test the sonar properly. To overcome this problem, further testing was performed in the Kerkpolder swimming pool. Due to the large area of the pool (50 by 25 m), sonar reflections on sides could be prevented. Moreover, the water depth could be adjusted manually ranging from 1 to 2 meters in depth.

The testing and monitoring in the natural environment, took place in the region Andalusia, Spain, during the period from mid-September to the end of October 2019. In Figure 23 the three measuring locations are indicated. Measurements were performed in two different river basins, respectively, the Guadalquivir and the Guadalete river basin. Both river basins discharge into the Atlantic Ocean and are subject to tidal conditions near the river mouth. The Guadalquivir river is the second largest river in Spain and starts at the Sierras de Cazorla (Más Spanje, 2019). It drains an area of 57,017 km^2 including Sevilla and a large part of the population in Andalusia, resulting in a high pollution rate (Blomquist, Giansante, Bhat, & Kemper, 2005). In the Guadalquivir river, monitoring took place at a platform about 5 kilometres North East of La Algaida (2). The Guadalete river originates in la Sierra de Grazalema and drains an area of 3677 km^2 (Ayuntamiento de Jerez, 2019). The Guadalete river is known as one of the most generally polluted rivers in Spain (Ayuntamiento de Jerez, 2019). In the Guadalete river basin, measurements were performed at two locations, in the Rio de San Pedro river, near Puerto Real (1) and the Guadalete river (3) at El Puerto de Santa Maria.
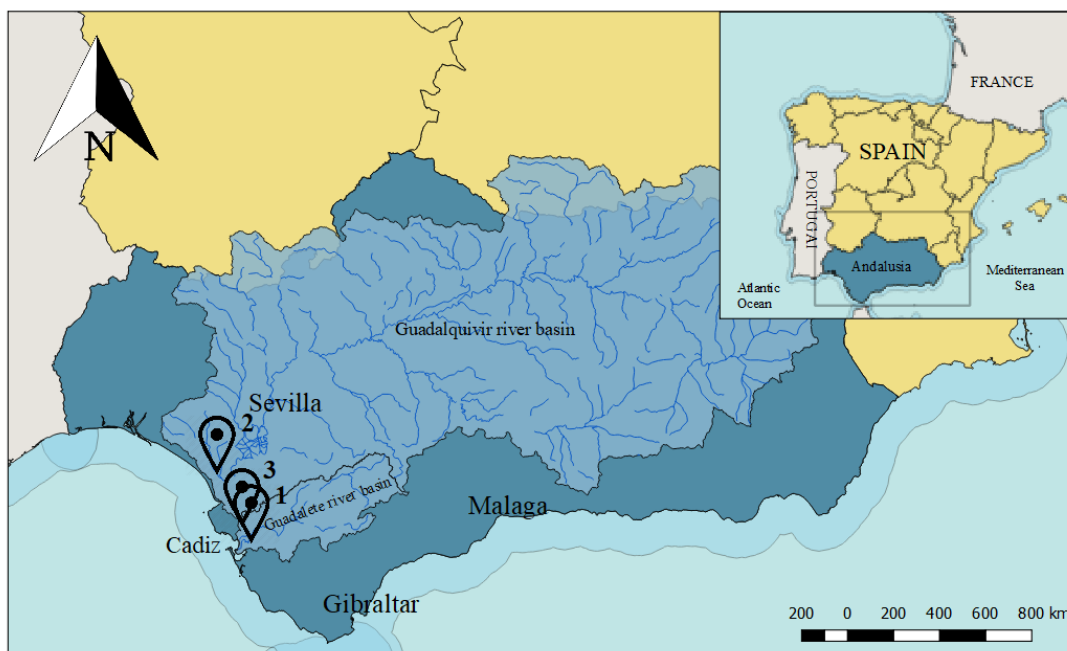

Figure 23: Study area and measuring locations 1 – 3 in Andalusia, Southern Spain.

3.1.3. Controlled tests in artificial environment

To get an insight into the scanning technique and detection abilities of the echosounder, experiments in the Kerkpolderbad in Delft were performed. The controlled, steady and relatively large environment of the swimming pool were the reasons to use it for the controlled tests. Taking theory into account, several factors can influence the sonar readings, such as rotation of the objects, flow velocity, and depth, which were separately investigated during these tests.

The experimental setup was as follows. The water depth of the pool was fixed at two meters depth. Two weights were placed at the bottom of the pool, 2.5 m aside from each other. Additionally, two lines were attached to the weights and fixed to the floating lines at the water surface. In between these vertical lines, two horizontal lines were located at 0.5 m depth and 1m depth from the surface. Just above the water surface, a line was fixed to attach the sensor to. The objects for the tests were dragged underneath the sensor using a rope. The experimental setup used is displayed in Figure 24. Moreover, the beam angle of the Deeper CHIRP+ was set to narrow (7 degrees) and the sensitivity to 100%. The narrow scanning beam was used since this beam provides the highest scanning resolution and smallest blind zone.
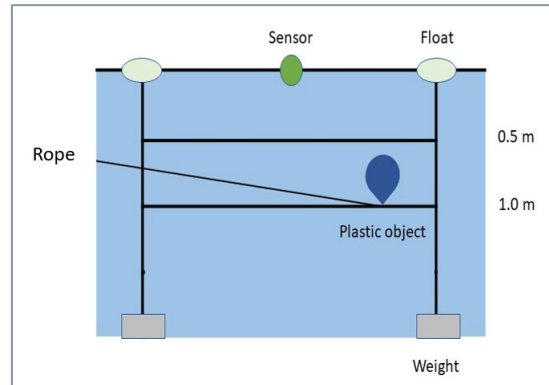

Figure 24: Experimental setup controlled tests in artificial environment (swimming pool Kerkpolder).

In accordance with fish finding theories and techniques, the focus regarding signal size followed three suppositions:

1) Signal size large item > signal size small item
2) Signal size object at large depth > signal size object at small depth
3) Signal size with low flow velocity > signal size with high flow velocity

Firstly, as mentioned before, the purpose of the test in the pool was to take variables influencing the sonar reading separately into account. Spherical items were used during the tests in the pool. In this way, the orientation of objects when passing the sensor was eliminated. As spherical non-floating items, balloons filled with water were used, pictures present in Appendix A).

Moreover, the influence of object size on the sonar readings was investigated. In order to answer the question of whether the size of the object can be determined by looking at the sonar readings, objects of different sizes were used. To this end, balloons of 8 cm and 15 cm diameter respectively were used during the tests in the controlled environment. The two balloons were repeatedly dragged underneath the sensor at equal depth and velocity of 0.5 and 0.15 m/s respectively.

Furthermore, since the echosounder is scanning in a cone, the scanned area near the bottom is larger than at the top of the water column. When objects are not fixed at certain depths, variations in displayed signal dimensions could be induced. It could also be the case that the sonar corrects for the depth itself. To test this, the balloons were fixed at two different depths, respectively 0.5 and 1 m below the water surface and repeatedly dragged underneath the sensor with a velocity of 0.15 m/s. The dragging velocity was set by dividing the fixed dragging distance by the dragging time.

Lastly, the influence of flow velocity on the sonar readings was investigated. It could be possible that the width of the displayed signal depends on the velocity at which the items are passing the sensor. If, for example, an object remains steady below the sensor, it is constantly displayed. Two different velocities, 0.15 and 0.25 m/s, respectively, were used for which the balloons were repeatedly dragged passing the sensor at 0.5 m depth.

The previously mentioned suppositions were tested using the following three sets of hypotheses:

I. H_0 The signal size is not related to item size
      H_1 The signal size is related to item size

II. H_0 The depth of the object does not influence the signal size
      H_1 The depth of the objects does influence the signal size

III. H_0 There is no relation between signal size and flow velocity
      H_1 There is a relation between signal size and flow velocity

The hypotheses were tested using the t-test. The results are shown in section 4.1.1 of the Results and Discussion Chapter.

Additionally, since during the tests with the spherical items (balloons), the rotation of objects was discarded, the possible influence of object rotation was tested separately. To investigate the impact of orientation on the sonar signal, a 1.5 L water bottle was used. The bottle was attached to the line at 1 m depth and rotated in horizontal direction for 30 seconds, remaining steady below the sensor. Thereafter this was repeated for the bottle positioned vertically. The scanning beamwidth was kept at 7 degrees and the sensitivity at 100%. After performing the tests, the sonar data was uploaded to Lakebook.

3.1.4. Semi-controlled tests in natural environment
Tests in a natural environment were executed at an existing platform in the Rio de San Pedro. The goal of this method was to investigate the abilities of the echosounder in the natural environment under semi-controlled circumstances. These tests were repeated at five days in October, on the 3rd, 10th, 14th, 25th and 29th to obtain a dataset needed for statistical analyses of signal size and signal strength.

In Figure 25, the experimental setup is illustrated. The echosounder was attached to the platform and was floating on top of the water. Targets were fixed to thin fishing lines and placed at approximately 0.5 m depth. The targets were released and passed the sensor, driven by the river's flow velocity. The time at which the target was displayed was noted. After the target passed the sensor, the target was removed from the water. Per target, the test was repeated ten times. For these tests, the narrow scanning beam and a sensitivity of 100% were used. The narrow scanning beam was used because, as stated in section 2.3.2, the narrow beam has the highest scanning resolution and the smallest blind zone of 15 cm, for which the sonar is not able to detect objects.
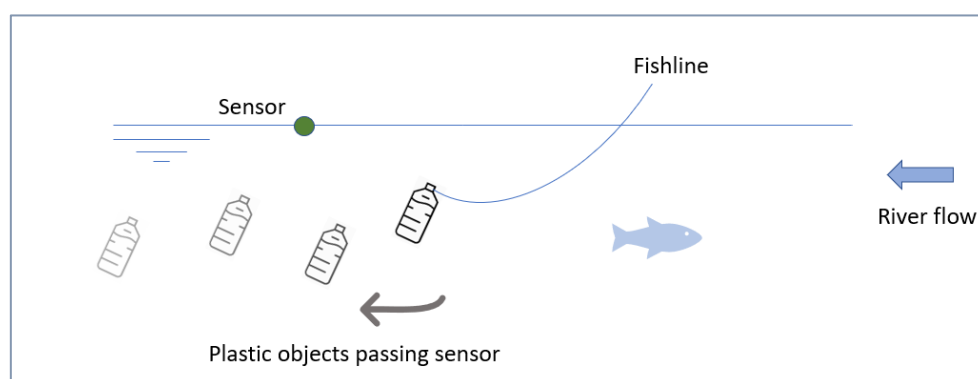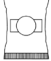

Figure 25: Experimental setup semi-controlled tests with targets in the Guadalete river.

Different targets were used for testing the plastic detection abilities of the echosounder. The targets were picked according to what could be found at the riverside itself, in combination with targets that commonly appear in the water column according to different studies (section 2.2.2). For the last two testing days, the set of targets was extended.

The following items were used for testing:

1) Hard plastic cup

2) Thin, transparent plastic bag

3) 33 cl aluminium can

4) 0.5 L plastic bottle

5) 1.5 L plastic bottle

6) Food wrapper large (20 cm)

   Extended set of targets:

7) Food wrapper small (12 cm)

8) Food container

Pictures and dimensions of the objects used can be found in Appendix B).

During the last two testing days (25th and 29th of October), flow velocity was measured before testing each target. Flow velocity was measured because, when analysing signals from previous testing days, it was apparent that signals for the same object differed over the various days. A possible reason could be the change in flow velocity over the testing days. Since tests were performed in a tidal river, the flow velocity varied significantly. To estimate flow velocity, a propeller was placed at 0.5 m depth in front of the echosounder. After one minute, the propeller was removed and the number of turns of the propeller was noted, from which flow velocity was calculated. After performing the tests, the sonar data was uploaded to Lakebook.

3.1.5. River monitoring (uncontrolled natural environment)

River monitoring was executed in two different river basins in Southern Spain. First, monitoring was performed in the Guadalquivir river, where the sonar was used simultaneously with two nets. In the Guadalete river monitoring took place from a pedestrian bridge. Both river monitoring practices are described below.

Monitoring in combination with nets

The echosounder was implemented during a monitoring campaign in the Guadalquivir river on the 3rd of October 2019. The goal of monitoring in the river, in combination with nets, was to test the sensor in the natural environment while being able to validate the sonar readings with the litter caught in the nets. The monitoring was executed when the river tide was going from high to low. In other words, litter coming from inland passed the sensor on the way to the sea. As a monitoring spot, an existing platform at the riverside was used.

The sensor was placed in front of two nets to validate the sonar readings. The two nets, with a mesh size of 4 cm, were located at the bottom and the water surface. The net at the water surface was 2.5 m wide and 0.8 m high, the net at the bottom was 0.8 m by 0.8 m. The beam angle of the Deeper CHIRP+ was set to the medium beam, 16 degrees, to cover approximately the same area as the nets. When using the medium beam, a blind zone of 60 cm is present at the water surface, as stated in section 2.3.2. Using the wide scanning beam was not feasible since the transmitted waves reflected on the platform's structure. Furthermore, the sensitivity of the senor was set to 100%. The experimental setup is illustrated in Figure 26.
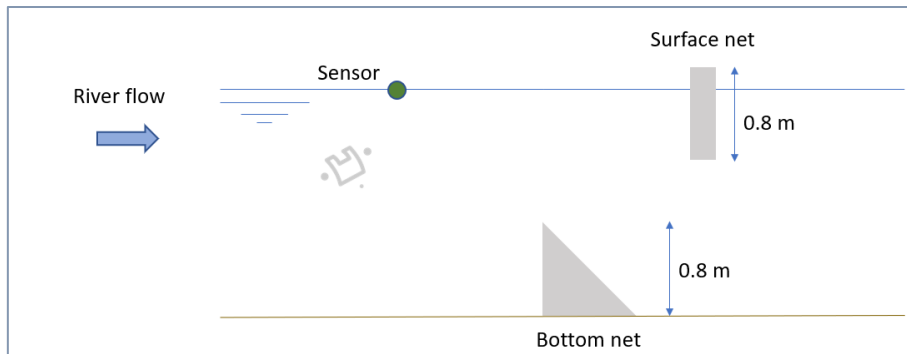
Figure 26: Experimental setup Guadalquivir river monitoring in combination with nets.

After three hours of consecutive sampling, the nets were taken out and the litter items were collected. The litter items were measured and grouped using the different plastic categories. The sonar readings were thereafter uploaded to Lakebook.

Monitoring Guadalete river
To apply the echosounder further in natural conditions to monitor plastic litter in the river, the sensor was operated during 18 hours of monitoring in the Guadalete river. The sensor was deployed from a pedestrian bridge, crossing the river, in El Puerto de Santa Maria. The monitoring took place at eight different days of varying tide conditions. Additionally, three locations over the cross-section of the river were monitored.

Figure 27 shows the monitoring setup at the pedestrian bridge, including the three locations. The beamwidth of the sensor was set to 47 degrees (wide beam) and the sensitivity to 100%. With the wide beam, the sensor scans with the highest spatial resolution, and is, therefore, able to detect most litter. However, a blind zone of 0.8 m at the water surface was present. The exact covered scanning area depends on the water depth at the time of monitoring. After each monitoring activity, the data was directly uploaded to Lakebook.
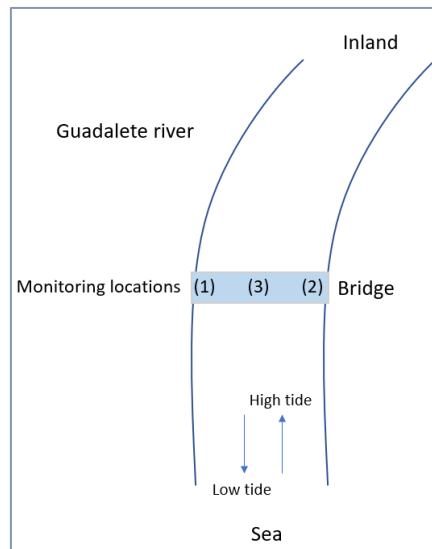
Figure 27: Setup Guadalete river monitoring from the bridge, with monitoring locations 1 - 3.

3.2. Data processing

In the previous section, the methods used for the data collection are explained. After data collection, the data was processed, which is elaborated on in this section. The general data processing actions, which were performed in MATLAB are provided. The specific data processing, for the three methods, is described separately.

3.2.1. General image analysis with MATLAB

The data obtained during the three different experiments were saved in Lakebook. Since there was no possibility to export raw sonar data or images from Lakebook, screenshots of the displayed signals were taken. These screenshots were imported to MATLAB as RGB images of unit8 format, an example image is provided in section 2.4. To investigate the ability of echo sounding to detect submerged plastics, potential relations were examined. These relations can be split into two categories, respectively, the size of a displayed signal and the intensity of a displayed signal. General steps, performed in MATLAB, regarding calculating the size and intensity of the sonar signals are described below and presented in Figure 28 and Figure 29.

To calculate the signal size, the images were first segmented to exclude the background pixels from the foreground pixels. Details on image segmentation, using K-Means clustering are provided in section 2.4. After segmenting the images, binary images were created in which pixels representing the sonar signal were indicated by the value 1 and background pixels by the value 0. The number of pixel rows and columns representing respectively the height and width of the sonar signal was determined. Since the width of the sonar signal is scaled on a time axis, the speed at which objects passed the sensor can influence the signal width. To correct for flow velocity, the width and height of the signals were calculated separately. The width was corrected for the flow velocity, whereafter the signal area was calculated. These steps are illustrated in Figure 28.
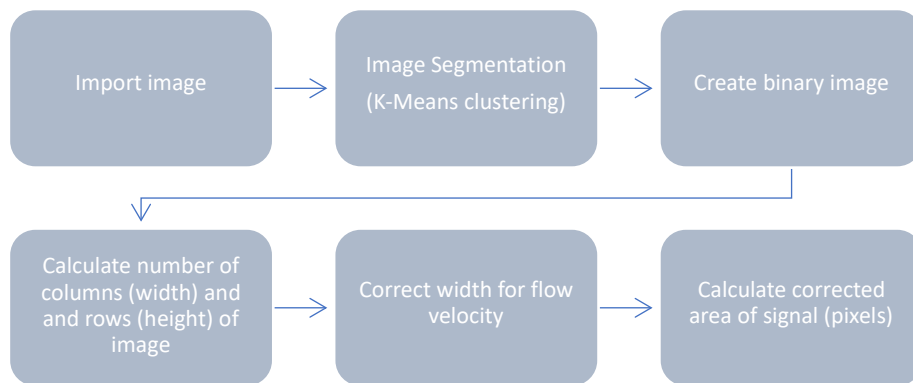
Figure 28: Steps performed for determining the size (pixels) of the sonar signal.

For calculating the signal intensity, the signal RGB images were split into the three channels, red, green, and blue. More information about RGB images is given in Chapter 2.4. After splitting the RGB channels, the background values were set to Not a Number (NaN). For each specific channel, the number of pixels present in the image was calculated, and the RGB colour component pixel values were calculated. An overview is provided in Figure 29.
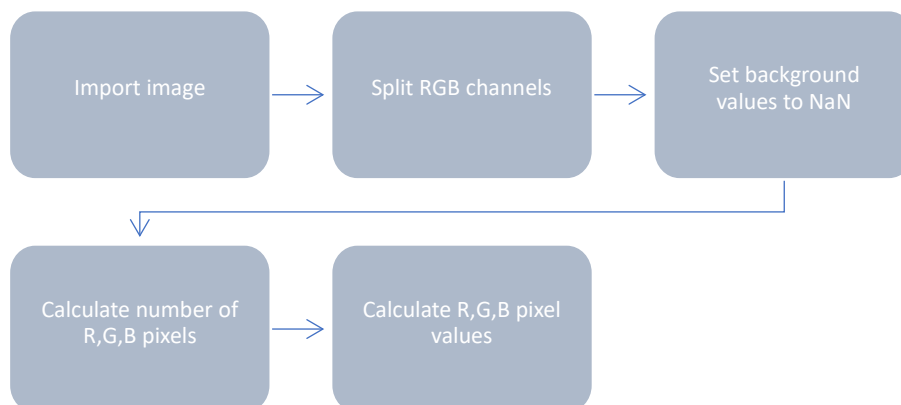

Figure 29: Steps performed for determining the sonar signal intensity.

After calculating signal size and intensity, statistical analyses to investigate potential relations were performed. The results per test are presented in the Results and Discussion Chapter. The specific data processing for the different tests is described in the sections below.

3.2.2. Data processing of the controlled tests in artificial environment

To examine the sonar signals, screenshots of the sonar signals in Lakebook were taken. A sonar reading obtained during the controlled tests, as presented in Lakebook, is shown in Figure 30. To process the data, first, the sonar signal area was calculated for the large and small balloon, for the same depth and velocity. According to the first hypothesis, the sonar signal dimension of the large balloon was compared to the signal dimension of the small balloon.

Moreover, the sonar signal dimensions were calculated for the tests with the large balloon at two different depths, for the same flow velocity. The influence of depth on the signal size was examined by comparing the two datasets obtained. Furthermore, the influence of flow velocity on sonar signal size was investigated by calculating and comparing the area of the sonar signal for the large balloon at two different velocities.

The significance of the results, whether the null hypothesis, regarding object size, depth, and flow velocity could be rejected or not was determined using a t-test. The t-test was performed with a significance level of 0.01, corresponding to a confidence level of 99%.
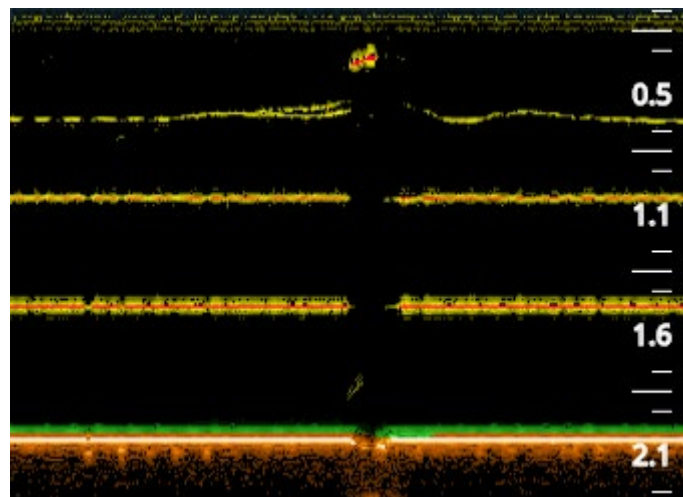

Figure 30: Sonar reading of the large (15 cm) balloon filled with water at 0.5 m depth, obtained from the controlled testing in the artificial environment.

Additionally, the impact of the orientation of an object on sonar signal size was examined. The signal height was calculated using MATLAB and compared for the horizontal and vertical bottle orientation. Besides, the calculated sonar signal heights were compared to the actual dimensions of the plastic bottle. The number of pixels in each column was calculated, representing the height, in pixels, of the sonar signal. To compare the sonar signal height with the dimensions of the 1.5 L bottle, the pixels were converted to a metric index. The pixel unit was converted into centimetres by determining the metric size of a single pixel, using the metric scale in the images and the amount of pixels present. The determined ratio is 1 pixel being 0.0111 meters.

3.2.3. Data processing of the semi-controlled tests in natural environment

Screenshots of the sonar signals were taken and grouped by target and testing day. Figure 31 and Figure 32 present parts of the sonar data obtained, as saved in Lakebook. For each testing day and target, the signal height and deviation of the signal height were calculated. Since the x-axis of the sonar reading represents time and not distance, the signal height was used as sonar signal size indication. For the measurements on the 25th and 29th of October (experiments 4 and 5), the signal width was corrected for the flow velocity measured, and signal areas were calculated. As previously mentioned, flow velocity was measured with a

propeller. The width of the signal was corrected for the flow velocity by multiplying the width with the flow velocity. This resulted in the corrected width w_c. The corrected area is now $A_c = w_c * h$. Furthermore, signal intensities were calculated per object, per day and compared over the testing days. The signal intensities were calculated using the RGB pixel values. The calculated signal intensities were used to investigate the relation between plastic type and sonar reflectance.
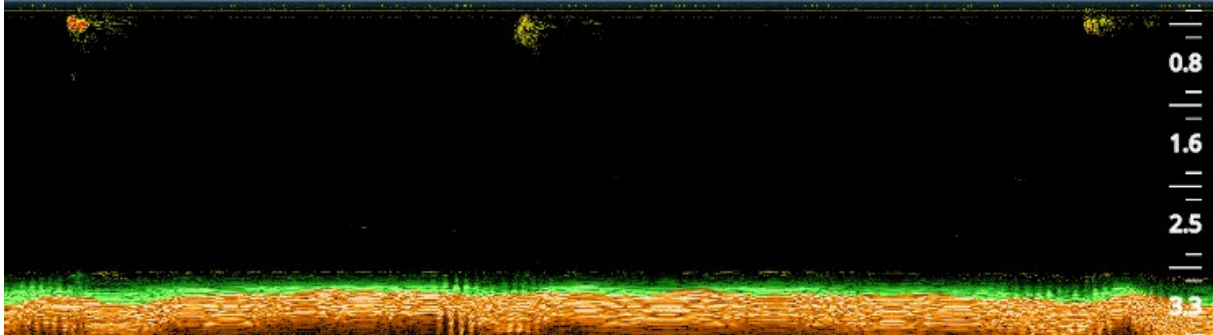
Figure 31: Sonar reading of passing a plastic film (thin plastic bag) for three times, obtained from the semi-controlled tests in the natural environment.
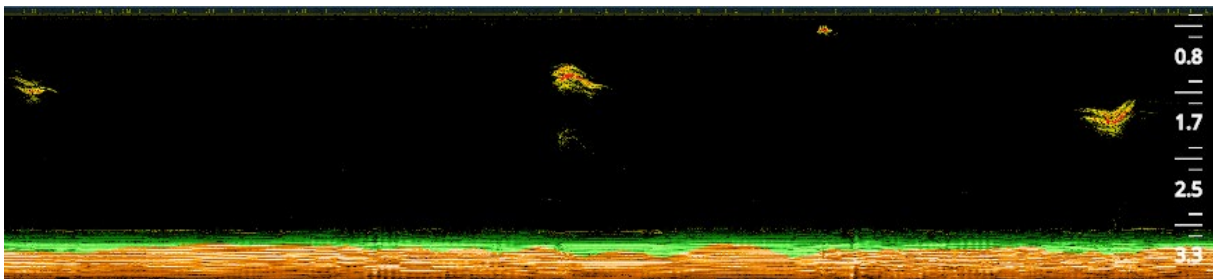
Figure 32: Sonar reading of passing an aluminium can (33 cl) for three times, obtained from the semi-controlled tests in the natural environment.

3.2.4. Data processing of the river monitoring (uncontrolled natural environment)

Monitoring in combination with nets

The sonar readings during the three-hour monitoring period were analysed. The number of items passing the sensor was counted. Thereafter, the number of items reflected on by the sensor was compared to the number of items caught with the nets. Moreover, screenshots of the sonar signals were taken and signal height and intensity were calculated. Figure 33 shows a detected item during the monitoring activity, as present in Lakebook. According to the outcome of the semi-controlled tests, relations between the sonar signals and the collected litter were investigated.
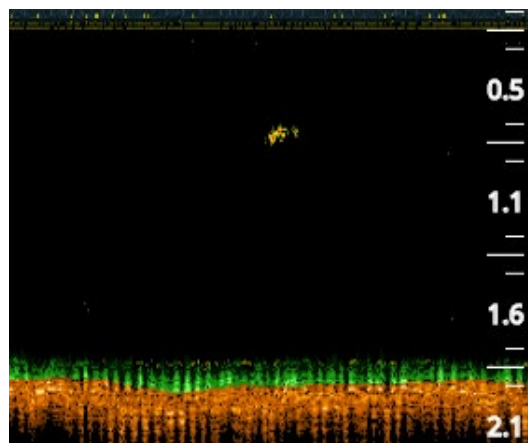
Figure 33: Sonar reading of an item that passed the sensor during the three hours of consecutive sampling in the Guadalquivir river in combination with nets.

Monitoring Guadalete river

During the 18 hours of monitoring in the Guadalete river, sonar data were collected for different sections of the river and varying river tide. The number of objects that passed the sensor per location and tidal condition was counted using the online platform (Lakebook). A sonar reading, obtained during the monitoring activity, including fish and a litter particle is provided in Figure 34. Relations between the number of detected items, tidal conditions and monitoring location were investigated.

The significance of the data regarding the number of litter items for incoming and outgoing river tide was determined using a t-test with a significance level of 0.01, corresponding to a 99% confidence level.
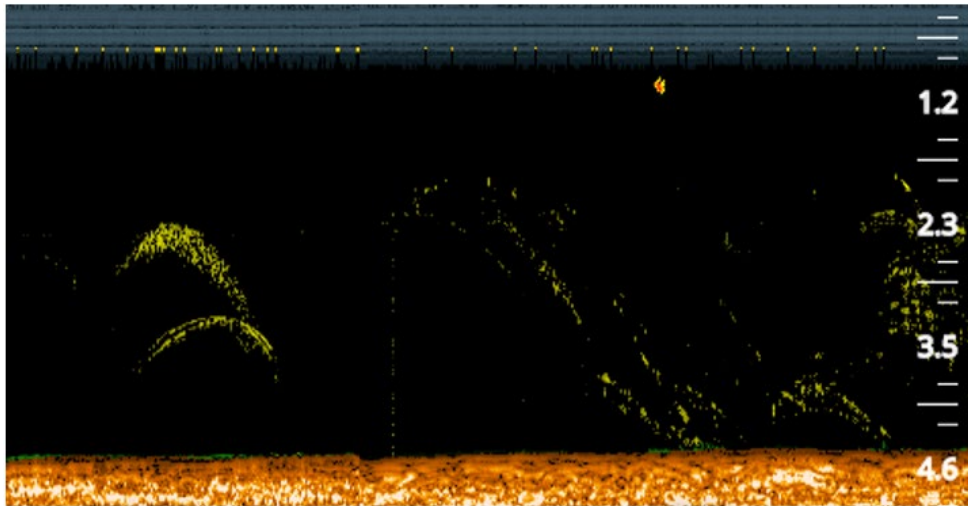
Figure 34: Sonar reading of litter monitoring in the Guadalete river. Fish presented by arches and a passing litter item at approximately 1 m depth.

Besides counting litter items, the position of the litter items over the river depth was also examined. The vertical position of the litter items detected was characterised using a division of the river depth into four equally spaced zones, as illustrated in Figure 35.

Figure 35: River depth divided into four equal zones for litter depth identification.

4.

Results and Discussion

In this chapter, the results obtained during this thesis are presented and discussed. First, the findings regarding the tests in the controlled environment are described. Secondly, the results of the tests with targets in the river system are provided and analysed. Finally, the outcome of the monitoring in the river system is presented and discussed.

4.1. Controlled tests in artificial environment

The aim of the tests in the controlled environment was to investigate the influence of flow velocity, depth, object size, and object orientation on the sonar signal. In section 4.1.1 the three hypotheses regarding flow velocity, depth and object size are tested and discussed. The influence of object orientation is tested separately, the results are presented in section 4.1.2.

4.1.1. Results testing hypotheses velocity, depth, and size

Regarding the above-mentioned variables, the following three sets of hypotheses were formed and tested. The underlying reasoning is explained in section 3.1.3 of the Methodology Chapter.

Hypotheses for datasets:
- IV. H_0 The signal size is not related to item size
         H_1 The signal size is related to item size

- V. H_0 The depth of the object does not influence the signal size
         H_1 The depth of the objects does influence the signal size

- VI. H_0 There is no relation between signal size and flow velocity
         H_1 There is a relation between signal size and flow velocity

Figure 36 presents the outcome of the tests in the controlled environment. Looking at the most left plot, the object size plot, the larger balloon shows a larger signal area than the smaller balloon. Moreover, in the second plot, where signal size for the two different depths is presented, no clear difference is observed. In the plot representing flow velocity and signal size, a difference in signal size between low and high flow velocities is noticed.
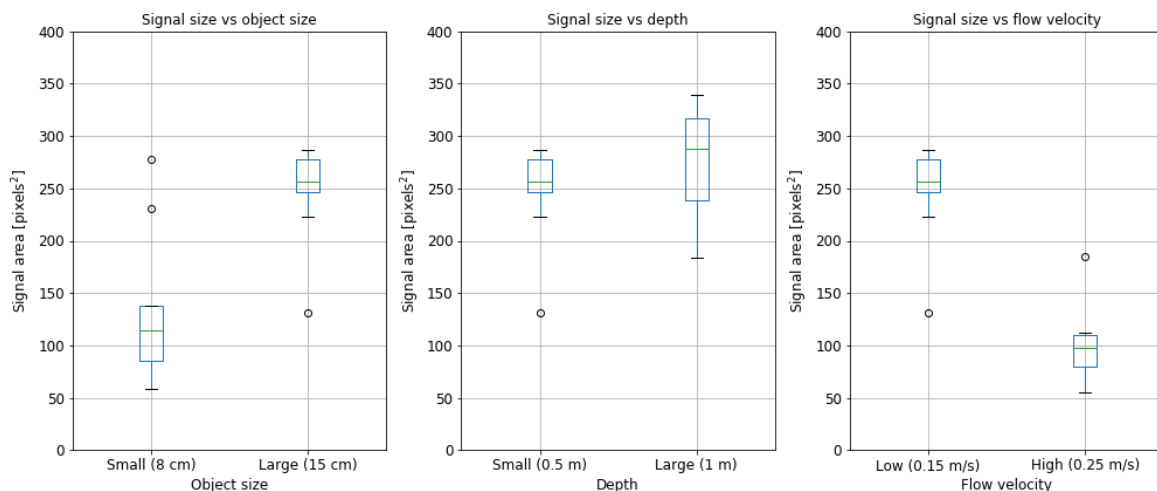

Figure 36: Test results controlled environment regarding the influence of object size, depth, and flow velocity on the sonar signal size, 25th and 75th quartiles used for boxplots.

To test whether the null hypothesis can be rejected or not, a t-test was performed with 0.01 as significance level. The calculated p-values for the three sets of data are shown in Table 5. Should the calculated p-value be less than or equal to 0.01, the null hypothesis (H_0) is rejected and the alternative hypothesis (H_1) is highly likely.

Table 5: Results testing hypothesis with independent t-test.

Dataset	Calculated p-value	Null hypothesis	Alternative hypothesis
I	0.01	Rejected	Highly likely
II	0.220	Not rejected	Not likely
III	0.00001	Rejected	Highly likely

Interpreting the results, taking into account the results of the t-test and Figure 36, it is indicated that a large item results in a larger signal than a small item. Moreover, the depth at which a similar object passed the sensor does not significantly influence the size of the signal displayed. Lastly, when objects are passing with higher flow velocity, the signal is displayed smaller than when items are passing with the lower flow velocity.

4.1.2. Results tests object orientation

The influence of the orientation of an object on the sonar readings was also investigated during the tests in the controlled environment. In Figure 37 the results of the tests with the 1.5 L plastic bottle are shown.

Figure 37: Signal height in pixels vs horizontal and vertical bottle orientation, 25th and 75th quartiles used for boxplots.

In Figure 37, it can be seen that when the bottle is held upright, vertically orientated, the height of the sonar signal is larger than when the bottle is orientated in the horizontal direction. When the number of pixels is translated to a metric index, using the found ratio of 1 pixel being 0.0111 meters, the vertically orientated bottle gives a median signal height of 10 cm, and the horizontally orientated bottle a signal height of 28 cm. The signal height in centimetres is shown in Figure 38, the median is presented by the orange line.
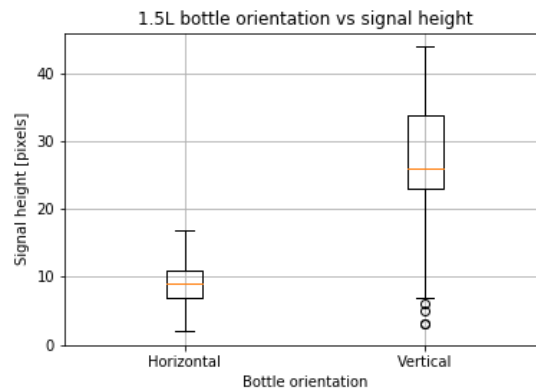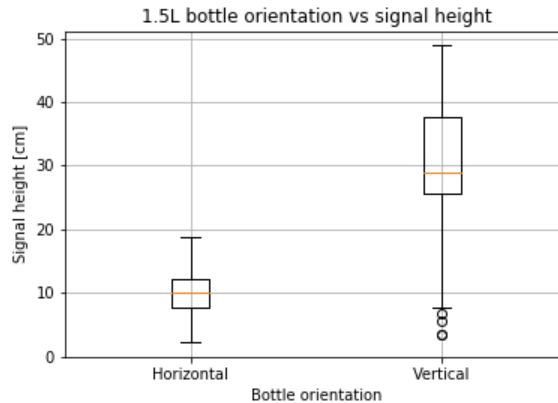
Figure 38: Signal height in cm vs horizontal and vertical bottle orientation, 25th and 75th quartiles used for boxplots.

When comparing the height of the sonar signal with the dimensions of the bottle, respectively 8.5 cm diameter and 27 cm high, the size of the bottle is overestimated by the sonar. However, the height of the sonar signal gives an indication of the vertical dimension of objects, and object orientation influences the displayed sonar signal.

4.1.3. Discussion controlled tests in artificial environment

Regarding the tests in the controlled environment, the following critical points can be noted. There are outliers present in the datasets, as indicated by the dots in Figure 36. These outliers may be caused by several factors. First of all, during the primary set of tests in the controlled environment, the balloons were dragged underneath the sensor with the use of a rope. Dragging the objects can influence the movement behaviour of the objects underwater. While dragging, a force is generated at which water is displaced in front of the object. This can affect sonar readings. The movement of water in front of the object can cause signal noise and reduced accuracy of the sonar readings.

Moreover, deformation of the balloons may occur due to dragging the balloons. Spherical objects (balloons) were chosen to eliminate object orientation and deformation. In this way, it was possible to focus on the influence of object size, depth and flow velocity independently. However, by dragging the balloons, especially at faster velocities, the balloon could deform. This may cause a range in the signal area for the different tests.

Furthermore, as can be noticed in Figure 36, there is no relation found between depth and signal size. It is possible that the algorithm used in the sensor corrects for this itself. During the tests, measurements were performed at 0.5 and 1.0 m depth. According to the shape of the cone at 7 degrees scanning beam, there should be a significant difference in the scanned area between these depths. However, further testing, at other depths could provide more insight to state whether depth is an influencing factor on signal size. During the tests, it appeared to be difficult to test at greater depth due to practical issues such as fixing the object to the ropes.

Additionally, the tests are performed for two different flow velocities, 0.15 and 0.25 m/s, respectively. The results show that flow velocity does influence the signal size. It appears that for higher flow velocity, the signal size is smaller. It is, however, not clear to what extent objects can still be detected with increasing flow velocity.

During the controlled tests, the narrow scanning beam was used. The narrow beam allows for scanning with the highest scanning resolution. However, this is paired with the lowest spatial resolution. By scanning with a cone of 7 degrees, the object has to pass the sensor at a specific location. Spreading of the data could be due to the item not passing the sensor in the centre of the beam but at the periphery. When the item passes the centre of the beam, a larger signal will be displayed than when an object only passes a part of the scanning beam. Since the data set is relatively small, the effect of the position of objects passing the beam could have a large

influence on the results. Besides, it is unclear if using the medium or wide beam would influence the results significantly.

When looking at the object orientation results, Figure 38, the vertical dimension of the bottle is clearly presented by the sonar signal. For this test, the bottle was held stationary underneath the sensor for a certain period of time. Since the sonar is scanning in pulses, the signal is divided into small intervals. This causes little gaps in the displayed signal. In MATLAB the signal is corrected by filling the main holes in the data, in order to obtain complete clusters but spreading in the results remains present.

4.2. Semi-controlled tests in natural environment

The outcomes of the tests with targets in the river system are presented below. There is a division made between the size of the sonar signal and the intensity of the sonar signal. First, the results regarding signal size for the different targets are presented. Thereafter the findings concerning signal intensity are provided. In section 4.2.3, the results of the semi-controlled tests are interpreted and discussed.

4.2.1. Results sonar signal size for the different targets

For the tests with different targets in the Rio de San Pedro, a set of eight objects, with different material properties, size, and shape were used. The signal height, in number of pixels, per object over the five different testing days is provided in Figure 39 and Figure 40.
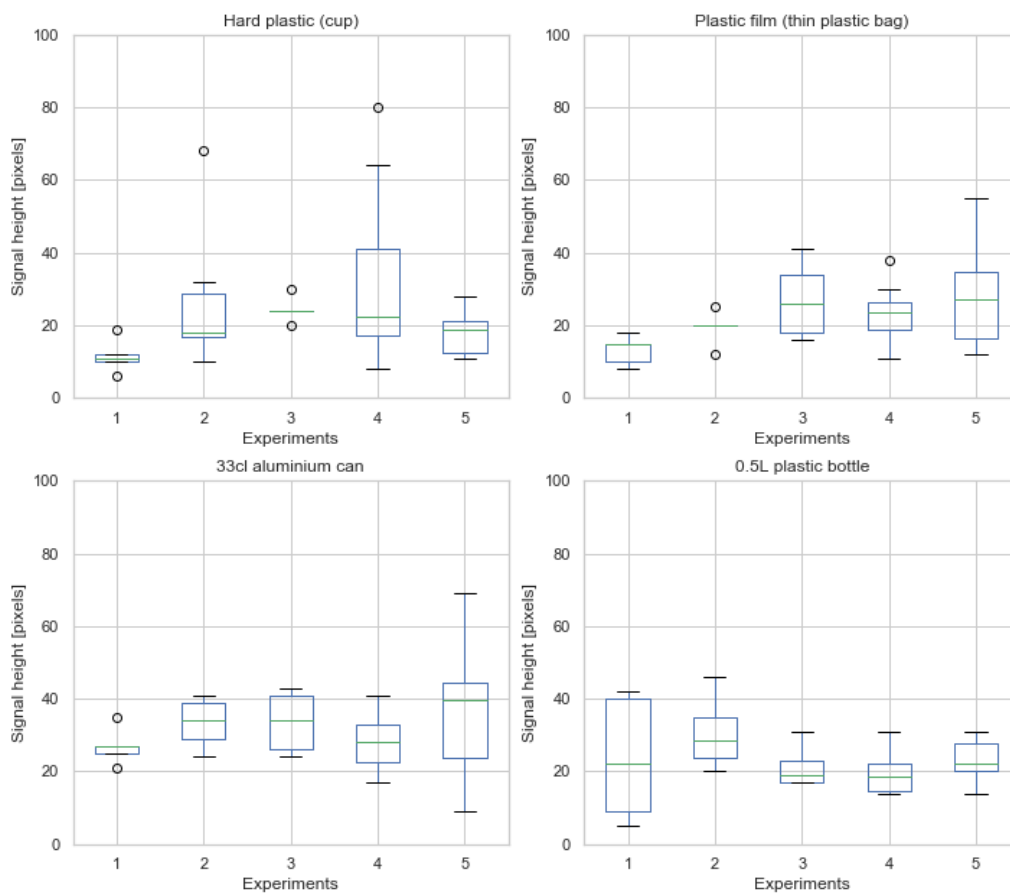
Figure 39: Sonar signal height in pixels for the items 1 - 4 over the five testing days (experiments), 25th and 75th quartiles used for boxplots.
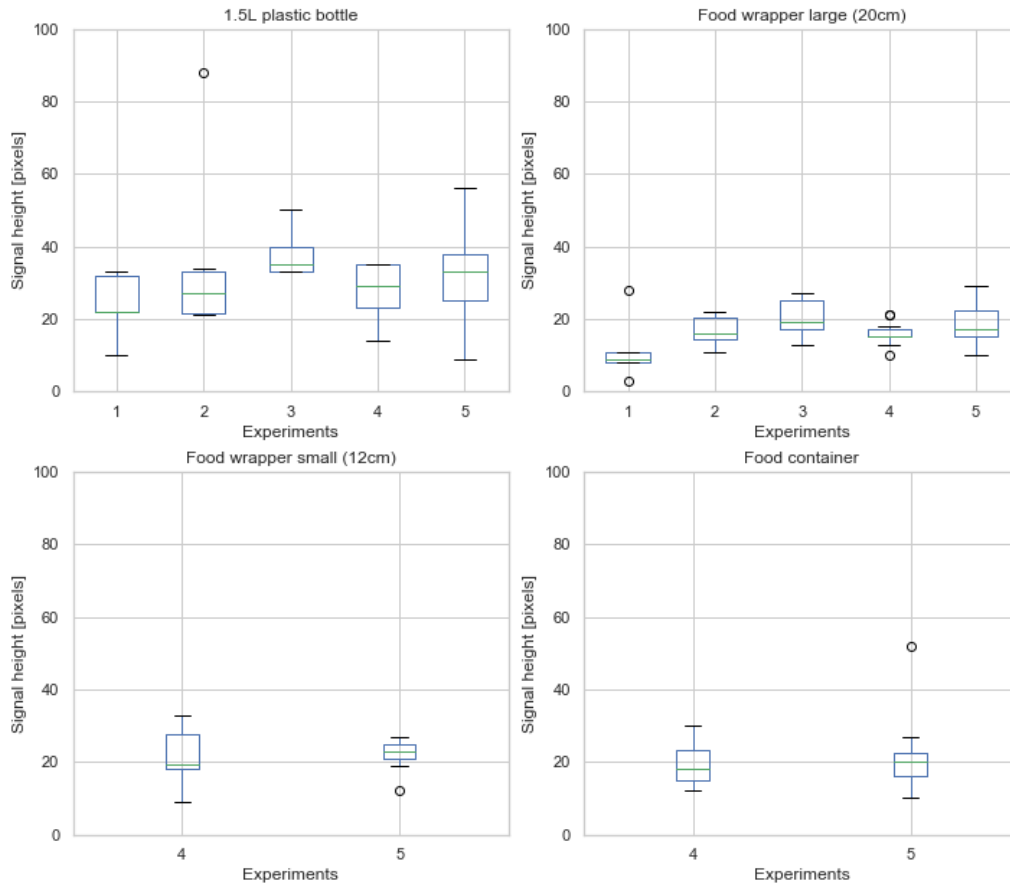
Figure 40: Sonar signal height in pixels for items 4 – 8 over the five testing days (experiments), 25th and 75th quartiles used for boxplots.

From the figures, it can be seen that the signal height per object differs over the testing days. The difference in signal size (height) may be due to several reasons, elaborated on in section 4.1.3. To look into the exact difference per object, the standard deviation per object for the experiments is presented in Table 6.

Table 6: Standard deviation related to signal height in pixels for the objects over the experiments.

Target	Standard deviation (pixels)
Hard plastic (cup)	16.53
Plastic film (thin plastic bag)	10.49
33cl aluminium can	10.94
0.5L plastic bottle	19.49
1.5L plastic bottle	31.63
Food wrapper large (20cm)	5.90
Food wrapper small (12cm)	6.30
Food container	9.15

From Table 6, Figure 39 and Figure 40, it can be observed that the 1.5 L plastic bottle has the largest standard deviation and the large food wrapper the smallest. To be able to compare the signal height of the targets, the averaged signal height of the experiments is presented in Figure 41.

Figure 41: Sonar signal height in pixels (log scale), per object, averaged for the different experiments, 25th and 75th quartiles used for boxplots.

From Figure 41 it is observed that the sonar signal height has a similar magnitude for the different objects. However, due to the presence of outliers, the visual comparison of signal height for the different objects is hindered. To be able to get a more detailed view, the results without outliers are presented in Figure 42.

Figure 42: Sonar signal height in pixels per object, averaged for the different experiments, without outliers, 25th and 75th quartiles used for boxplots.

As can be seen in Figure 42, the median signal height is the largest for the largest object, the 1.5 L plastic bottle. Differences between signal heights for the objects are, however, small. The 33 cl aluminium can is also displayed by the sonar as relatively large, with respect to its actual size.

Besides the signal height, also the signal area was calculated for the different objects. In order to determine the signal area, flow velocity measurements were used. Since flow velocity measurements were only available for experiments 4 and 5, the other experiments are not taken into account in the graphs below. As explained in section 3.2.3 in the Methodology Chapter, the signal width was corrected for flow velocity, since it is most likely that flow velocity influences the signal width.
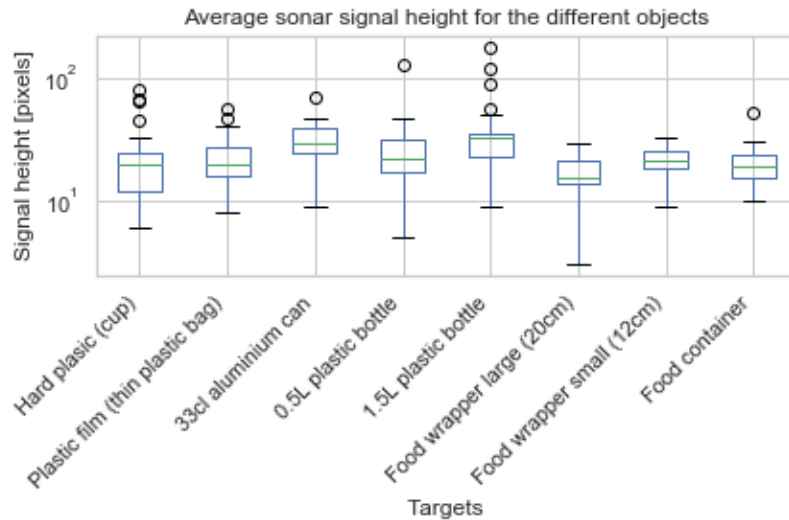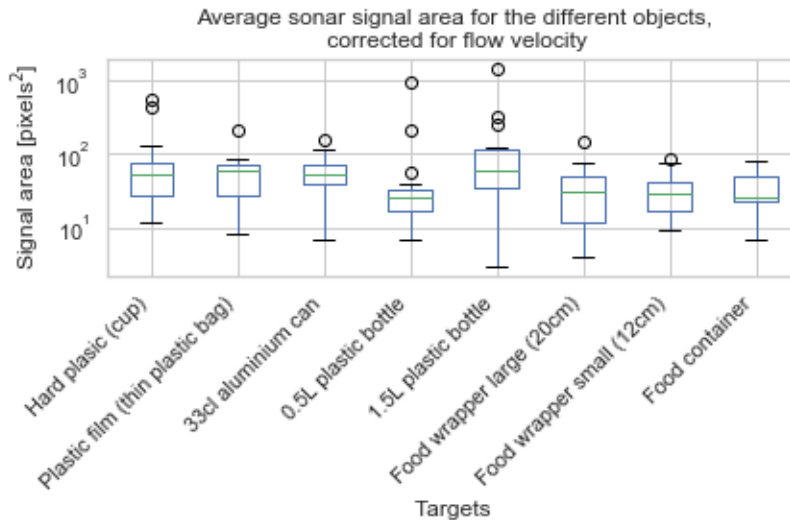
Figure 43: Sonar signal area in pixels (log scale), per object, averaged for experiments 4 and 5, 25th and 75th quartiles used for boxplots.

It can be observed that the results for the sonar signal area differ slightly from the sonar signal height results. However, no substantial differences in the signal area for the various objects are noticed. More insight is obtained when looking at the signal area, corrected for flow velocity, without outliers, presented in Figure 44.
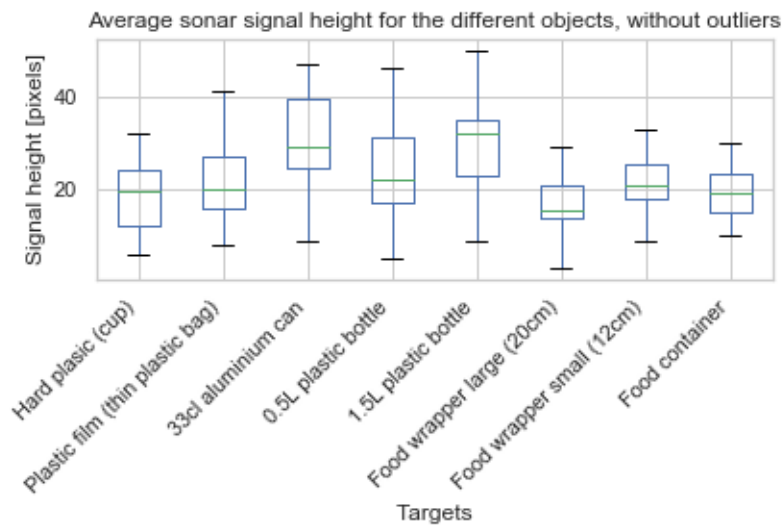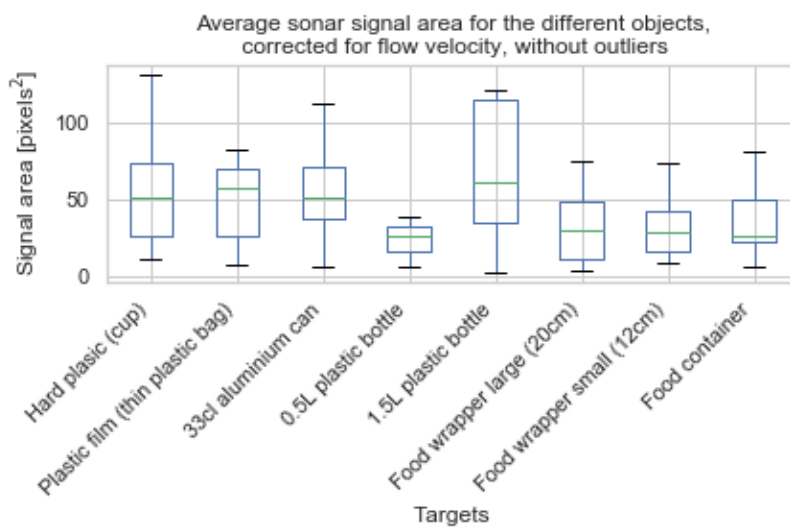

Figure 44: Sonar signal area in pixels, per object, averaged for experiments 4 and 5, without outliers, 25th and 75th quartiles used for boxplots.

From Figure 44, it can be seen that the 1.5 L plastic bottle causes the largest sonar signal. The range of the values, illustrated by the boxplot, is however substantial. Besides, the results taking only signal height into account differ from the results looking at the signal area. However, the datasets for both are dissimilar since for the signal area only the last two testing days are taken into account.

From the presented results regarding signal size for different objects, it is observed that different objects provide different signals. However, the differences between signals for the objects are small. In reality, the 1.5 L bottle is the largest object, when looking at signal height and signal area graphs this can be verified. Remarkable is that the aluminium can corresponds to a relatively large sonar signal. Possible reasons concerning the state of the data are mentioned in 4.2.3.

4.2.2. Results signal intensity for the different targets

Besides considering the dimensions of the sonar signals, the signal intensity of the sonar readings was also examined. As explained in the Theoretical background, the signal images are RGB images. The maximum and number of RGB values for each image are calculated using MATLAB and presented in the graphs below in Figure 45 and Figure 46.

Figure 45: Red, Green, Blue colour component values for items 1 - 6, averaged over the experiments.
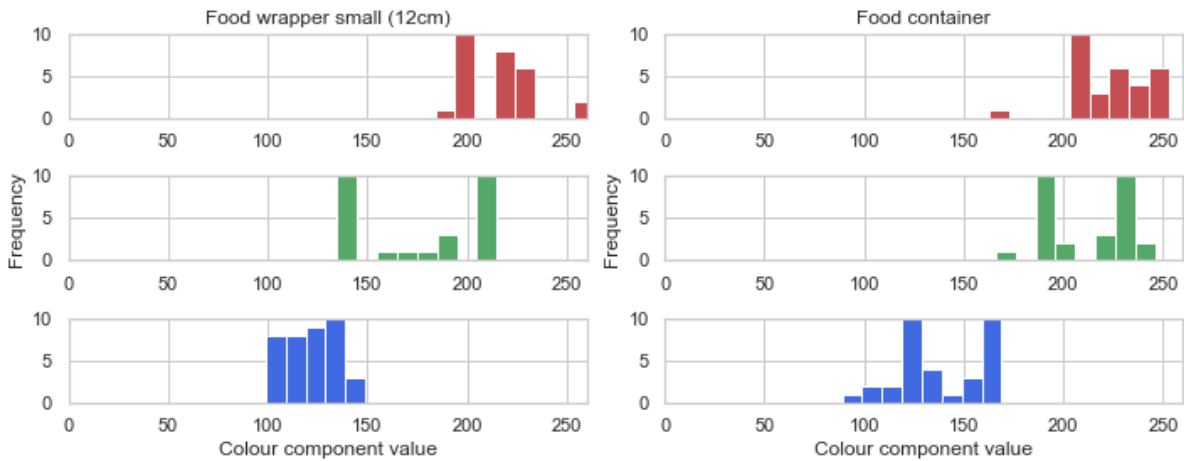
Figure 46: Red, Green, Blue colour component values for items 6 - 8, averaged over the experiments.

From Figure 45 and Figure 46, patterns in red, green, and blue colour component values were investigated. It can be observed that the RGB component values of the hard plastic cup are more distributed compared to the RGB component values of the other objects. Looking at the red colour component values, the data has the smallest distribution for the plastic film. Both the small food wrapper and the food container graphs are based on fewer data and cannot easily be compared to the other objects tested. Moreover, the 1.5 L plastic bottle shows more distribution in the data for the red and green colour components than the 0.5 L plastic bottle.

In Figure 47 and Figure 48, the minimum, maximum and average RGB component values for the different objects tested are illustrated.
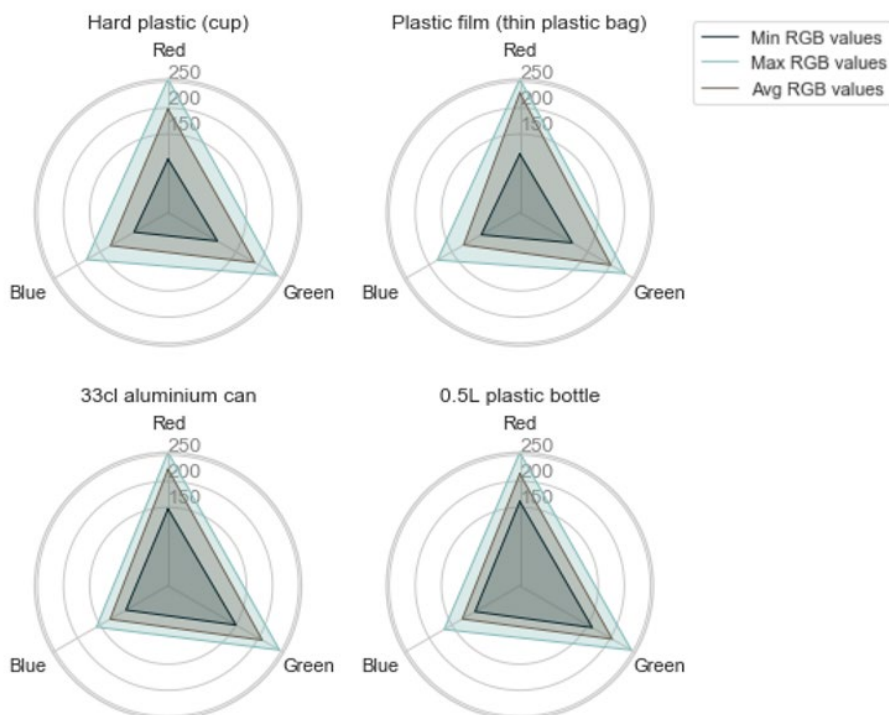
Figure 47: Radar plots of the minimum, maximum and average RGB colour component values for items 1 - 4.
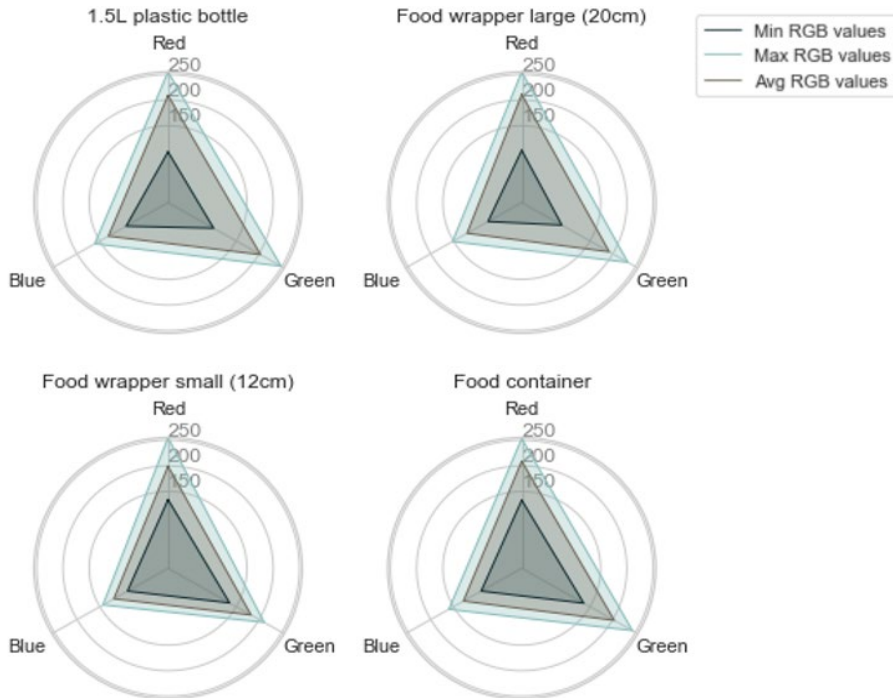
Figure 48: Radar plots of the minimum, maximum and average RGB colour component values for items 4 – 8.

From the figures, it is noticed that the spreading of the signal intensity values (the difference between the minimum and maximum values) is relatively large for the hard plastic cup, the plastic film, the 1.5 L plastic bottle, and the large food wrapper. Furthermore, the maximum RGB values for the objects differ only slightly. The maximum values considering the red colour channel are almost similar for the different objects. Some slight differences in maximum values considering the green and blue colour channels are observed between the objects. Regarding the minimum colour component values, differences between the objects are present. The large food wrapper results in the lowest minimum and the 0.5 L bottle in the largest minimum values.

In Figure 49 and Figure 50, the RGB colour component values are summed and averaged. Since signal intensity is displayed by the RGB colours. The RGB intensity can give an estimation of the signal intensity or strength.
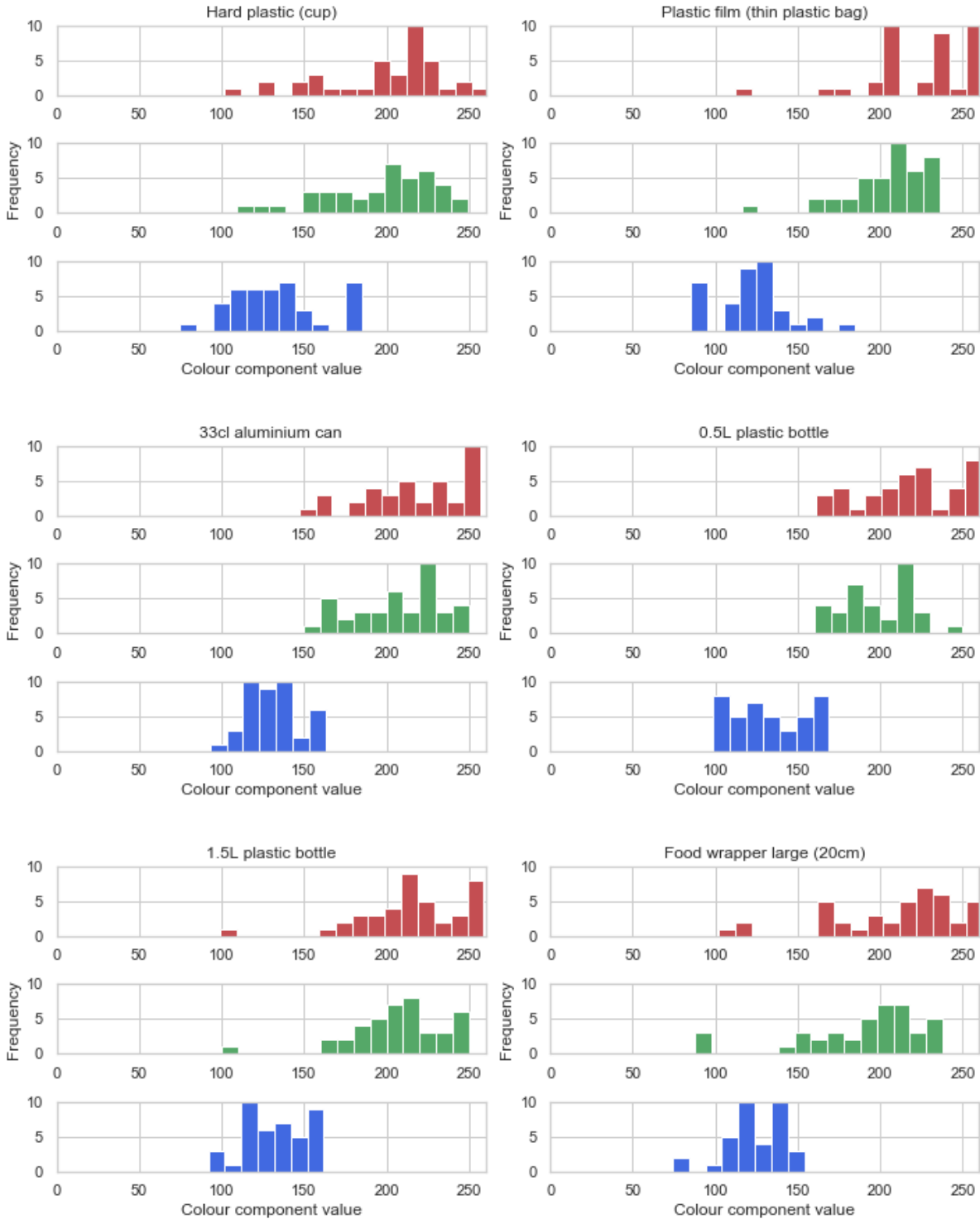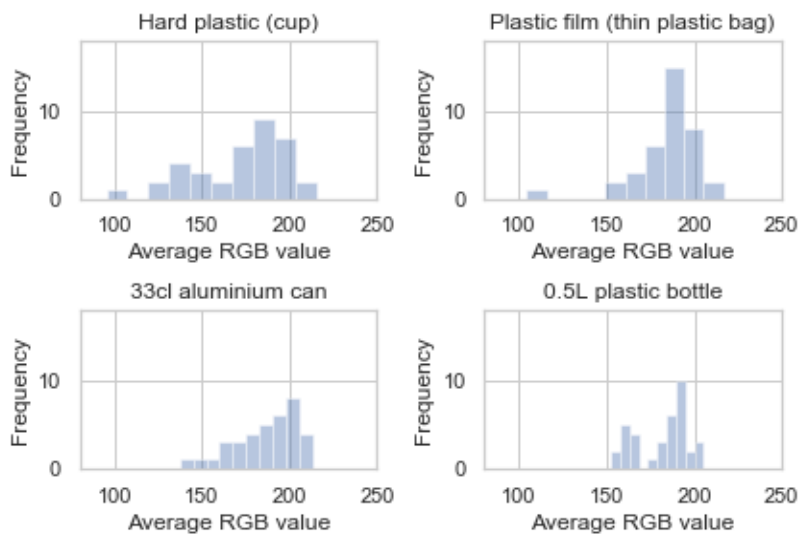

Figure 49: Averaged RGB colour component values for items 1 - 4, averaged over the experiments.
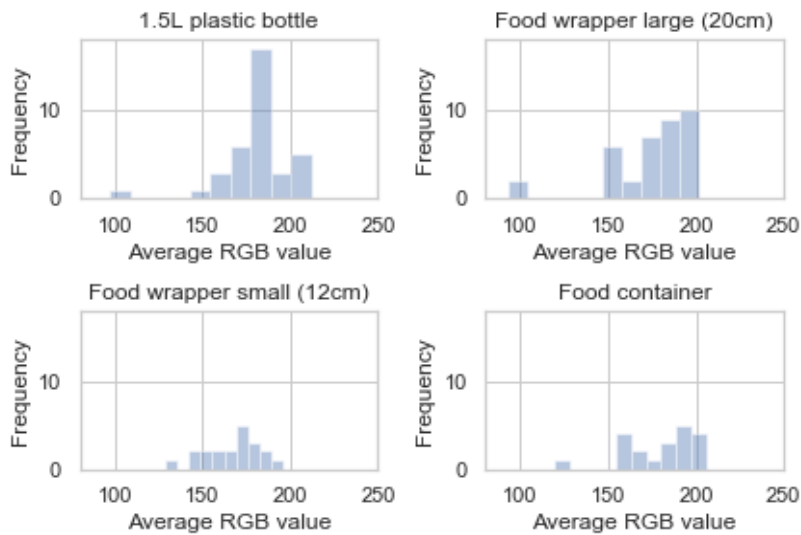
Figure 50: Averaged RGB colour component values for items 4 - 8, averaged over the experiments.

According to Figure 49 and Figure 50, relatively small differences in average max RGB values for the different objects are observed. Moreover, it is noticed that the aluminium can corresponds to the highest average RGB value and the large food wrapper to the lowest average RGB value. In order to compare the signal intensity with the material properties of the objects used, a division in material properties was made as presented in Table 7.

Table 7: Material type and density of the objects used.

Object	Material type	Density *(g/cm³)*
Hard plastic cup	PE-HD /PS	0,93-1,04
Thin transparent plastic bag	PE-LD	0,91-0,94
Aluminium can	Al	2,7
Plastic bottles	PET	1,37-1,45
Food wrappers	PE-LD	0,91-0,94
Food container	PP	0,9-0,95

When comparing the measured sonar signal intensities to the material properties, it can be recognised that for some objects the measurements fit the expectations, illustrated in Table 8.

Table 8: Sonar signal intensity of the used objects, ordered from high to low intensity, according to the measurements and material properties.

Order sonar signal intensity according to sonar data	Order expected signal intensity according to material density
Aluminium can	Aluminium can
Plastic film (thin plastic bag)	Plastic bottles
Plastic bottles	Hard plastic cup
Food container	Food container
Hard plastic cup	Plastic film (thin plastic bag)
Food wrappers	Food wrappers

When considering the order of the objects as presented in Table 8, it was noticed that the aluminium can corresponds to the highest signal intensity and the food wrappers to the lowest intensity. However, according to Table 8, no direct link between the sonar signal intensity and the material properties was found.

4.2.3. Discussion semi-controlled tests in natural environment

Regarding the displayed sonar signal size, a spreading was observed in the signal height over the different experiments/days, Figure 39. There are, however, relatively small differences between the recorded signal heights for the various objects. Factors that could cause the inconsistency of the sonar signal height over the days are temperature, salinity, and pressure. As stated in the Theoretical background, the soundwave velocity in saline water depends on these factors. Since tests were performed over five days in a tidal creek, the previously mentioned factors could have been different. The potential differences in soundwave velocity caused by changes in temperature, salinity, and pressure, as stated in the Theoretical background, may lead to the inconsistency in the results. However, for the conditions that applied during the measurements, the change in soundwave velocity is relatively small compared to the potential changes. To elaborate on this, the depth (pressure) ranged only between 2 – 7 m during the measurements, leading to a negligible change in soundwave velocity. The water temperature was between 20 and 25 °C, related to a soundwave velocity of 1527,17 and 1539,74 m/s, respectively. This could potentially have led to small differences in litter detection abilities of the echosounder. Since the salinity was not measured, only the potential change can be considered. As stated in the Theoretical background Chapter, the potential change in soundwave velocity considering salinity is 17 m/s. With respect to the soundwave velocity in saline water, of approximately 1533 m/s, a change of 17 m/s would only have a small impact.

The variance in the signal height for the objects itself could be due to diversity in object orientation. When objects are transported by the flow velocity of the water, their motion is not fully restricted. Inducing the objects passing the sensor orientated differently each time. In Table 6, the standard deviation of the signal height per object is presented. The 1.5 L plastic bottle data has the highest standard deviation. Since the 1.5 L bottle is the largest of the used objects, the influence of orientation on the signal height can potentially be largest, explaining the high standard deviation. In other words, the influence of object orientation of the 1.5 L bottle is expected to be larger than for smaller objects. Accordingly, the small food wrapper should then have the lowest standard deviation, if this is directly linked to object size. This was not the case for the test results. Moreover, the standard deviations of the different objects are quite similar.

Another possible cause of the deviation in signal size could be the deformation of objects. This holds especially true for the plastic bag, food wrappers, and possibly also for the food container. According to the material properties of the mentioned objects, their shape can change due to being transported by the river. The resistance to deformation of the other objects (cup, can, and bottles) is larger. However, the impact of orientation, as explained above, would possibly be larger for these objects.

Besides object orientation and deformation as possible causes for the deviations in sonar signal size, also the specific location at which an object passes the scanning cone could play a role. Looking at the scanning cone from the top, the xy-plane, the object can move through the cone in different ways. When an object travels through the centre of the plane, a larger signal will probably be recorded compared to when an object only travels partially through the plane. This could lead to differences in displayed object sizes. For single beam echosounders, it is not feasible to get an indication at which point objects passed in the xy-plane.

Considering especially the signal area of the objects (Figure 44), the suggested reasons for the deviation in signals apply as well. Additionally, to indicate signal area, flow velocity had to be taken into account. As stated in the Theoretical background, the height of the signal is represented in pixels related to a metric scale. The pixels indicating the width of the signal are related to a time scale. Therefore, to obtain signal widths, the data were corrected for flow velocity. The flow velocity was measured using a propeller and changed significantly in the tidal creek where the measurements were performed. The results differ compared to the signal heights. This could be because the flow velocity was only measured during the last two experiments, so the dataset is smaller compared to the signal heights dataset.

In general, regarding signal size, the 1.5 L plastic bottle is represented as the largest object in the data, as was expected. The aluminium can is also related to a large signal, larger than expected when looking at the actual size. This can be caused by the material properties, which can influence the reflectiveness of an object and possibly the displayed sonar signal size. The overall signal size data is, however, spread and no significant differences in signal size between the tested objects were observed.

Taking into account the obtained results regarding signal intensity, the following remarks can be made. From Figure 45, Figure 46, Figure 47, and Figure 48, illustrating the signal intensities by separate RGB colour channels, no clear relation for the objects was noticed. The average signal intensities related to material properties, provided in Table 8, are partly as expected. The aluminium can signal has the highest intensity, compared to the other objects, which is in accordance with its material property. The food wrappers are associated with the lowest signal intensity, which corresponds to their material properties. In contrast, the signal intensity of the thin plastic bag is higher than expected. This could be due to the entrapment and presence of air. Air reflects sound very well (Theoretical background) and could increase the reflectivity and so the signal intensity of the thin plastic bag. However, the difference in intensity values between the objects is small.

4.3. River monitoring (uncontrolled natural environment)

In this section, the results regarding the river monitoring are presented. First, the outcome of the monitoring in the Guadalquivir river in combination with nets is provided. Thereafter, the detected litter items for the 18 hours of monitoring in the Guadalete river are shown. The results of both monitoring activities are discussed in section 4.3.3.

4.3.1. Results monitoring in combination with nets

In accordance with the three-hour monitoring activity, as described in the Methodology Chapter, items, as presented in Table 9, were counted. For the sake of this research, only litter items of 2.5 cm and larger in the nets are taken into account. Images of the objects are provided in Appendix C).

Table 9: Number of monitored litter items in the Guadalquivir river for the echosounder and nets.

Monitoring technique	Monitored litter items
Echosounder	7
Surface net	6
Bottom net	1

As can be observed from Table 9, the signals obtained from the sensor do fit the number of objects found in the net. In Table 10, the signal height in pixels and centimetres and the signal intensities of the detected items are displayed. Only signal height is taken into account since the signal area depends on flow velocity. Comparison is made between the sonar signals and the items caught in the nets. The size of the items found in the nets is provided in Table *11*.

Table 10: Sonar signal properties of the detected litter items in the Guadalquivir river.

Item	Sonar signal height (pixels)	Sonar signal height (cm)	Signal intensity (av RGB value)
1	1.43	1.59	166
2	1.45	1.61	187.33
3	4.0	4.44	167.33
4	1.0	1.11	174.33
5	3.24	3.60	167
6	3.4	3.78	183.67
7	5.14	5.71	169

Item dimensions W – H – T (cm)	Item material properties
11 – 11 – 0.1	Plastic film
4 – 5 – 0.1	Plastic film
5 – 4 – 0.2	Food wrapper
7 – 8 – 0.1	Plastic film
1 – 13 - 1	Hard plastic
16 – 8 – 0.1	Plastic film
4 – 2 – 0.2	Rubber band

Regarding object size, the order of magnitude of the actual object size and the dimensions of the sonar signal are similar. However, no direct link between the sonar signal dimensions and the actual sizes of the caught litter was observed. According to signal intensity and item properties, the rubber band and hard plastic could potentially relate to respectively the highest and second highest signal intensity. Moreover, four approximately similar intensities are noticed, possibly indicating the plastic film items.

4.3.2. Results monitoring in Guadalete river

The results of the 18 hours of monitoring in the Guadalete river are presented below. The monitoring took place over eight different days, with varying tide and locations over the cross-section (1,2,3). The number of items per hour detected by the sensor is indicated in Figure 51.
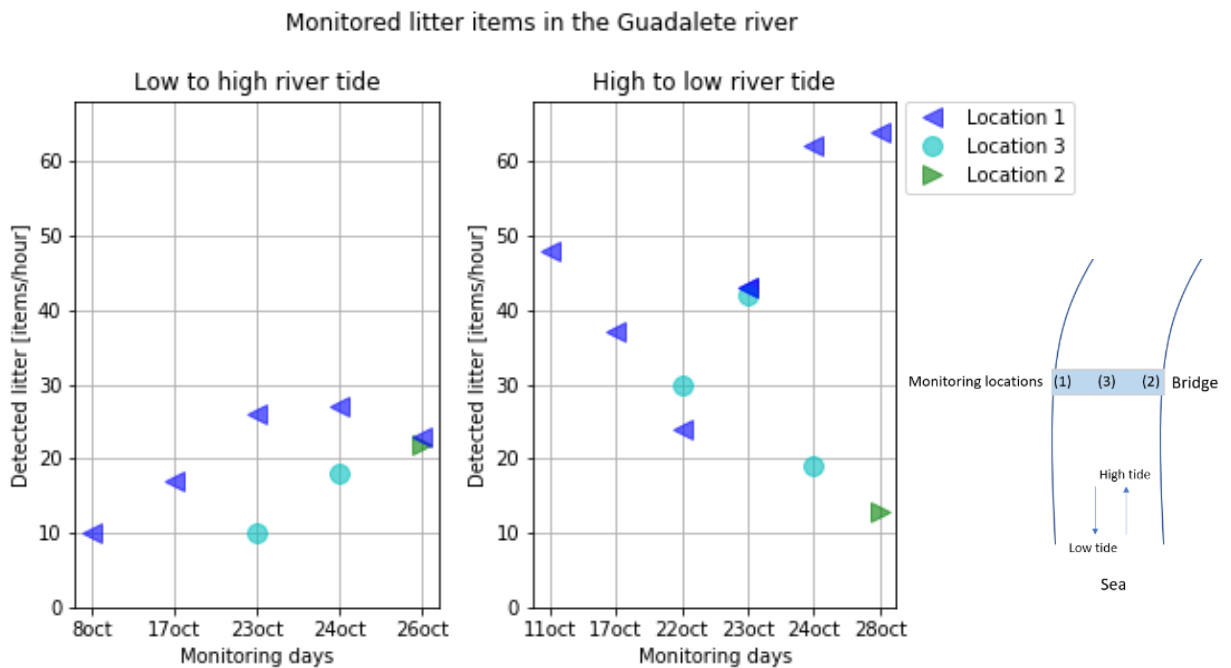
Figure 51: Monitored litter items per hour in the Guadalete river for varying tide and locations in the cross-section.

From Figure 51 it is observed that generally more items are transported when the river tide is going from high to low (water flows from inland to the sea), compared to the river tide going from low to high (water flows from the sea inland). The significance of this result is tested using a t-test with 0.01 as significance level. According to the calculated p-value of 0.009, it is determined that the number of litter items counted for incoming and outgoing river tide differs significantly.

On average, during flood tide (low to high river tide), 19 items/hour were detected by the sensor. For ebb tide (high to low river tide), 38 items/hour were detected. Moreover, the number of detected litter items differs over the monitoring days. Besides, a difference in monitored litter items over the cross-section was noticed. It appears that more litter is transported at location 1 compared to locations 2 and 3. In order to find an explanation for the difference in litter transport over the cross-section, the cross-section of the river was measured using the echosounder and is displayed in Figure 52. The left side of the displayed cross-section corresponds to monitoring location 1, the right side to monitoring location 2.

Figure 52: Guadalete river cross-section at the monitoring location, measured using the Deeper CHIRP+.

According to the measured river cross-section, it can be noticed that the river bottom is not uniformly shaped over the width of the river. Larger river depth is present at the left side of the river compared to the right side of the river (when looking upriver). In the next section, an elaboration on the link between plastic transport and river conditions is given.

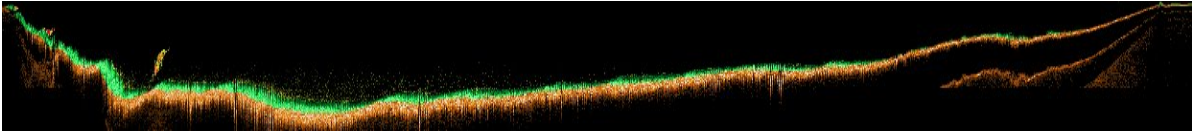Besides counting litter items, the depth at which the litter particles were present was also indicated, resulting in the particle distribution as illustrated in Figure 53.
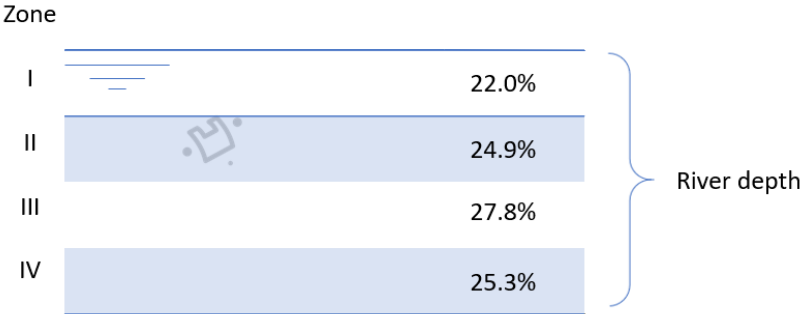
Figure 53: Division of the total monitored items over the river depth.

According to the figure, it is noticed that most litter items were present in the third zone. Moreover, it shows that the distribution of the detected particles is approximately uniform over the river depth.

4.3.3. Discussion river monitoring (uncontrolled natural environment)

Regarding riverine litter monitoring in combination with nets, some attention should be paid to the following matters. During the monitoring activity, it was unclear when each item caught in the nets passed the sensor. Items passing the sonar could be counted, however, they could not directly be related to the items found in the nets. This leads to difficulties in comparing the sonar data and the litter caught in the nets. The sonar signal size data and the actual litter size are not clearly related. Objects could have passed the scanning beam only partly or could be orientated differently than measured, leading to uncertainties in the sonar signal size. The sonar signal intensities could potentially be linked to the material properties of the caught litter items. However, differences in observed intensities are small, indicating uncertainties.

Moreover, the medium scanning beam was used to cover approximately the same area as the nets. However, when using the medium scanning beam, a blind zone of 60 cm at the water surface is present. This leads to a deficit in sonar readings for a substantial area at the top of the water column, where the surface net was present. The fact that a similar amount of items was counted from the sonar readings as was caught with the nets is likely to be a coincidence.

Furthermore, only a few items were collected during the monitoring activity. To be able to test the sensor more thoroughly, more litter items passing would be beneficial.

During the monitoring in the Guadalete river, the wide beam with the highest spatial resolution was used for scanning. However, this induces a lower scanning resolution and a blind zone of 80 cm. Objects passing above 80 cm water depth could not be detected. Regarding the plastic distribution over the cross-section of the river. There was only measured at 3 locations, not covering the entire river width. However, there seems to be a difference in litter transport over the cross-section. In the outer bend, at location 1, according to the data, more litter was transported compared to the other two locations. A possible reason could be the shape of the river, specifically the bend which is present. In the outer bend, flow velocities are generally higher, leading to potentially more items passing than in the inner bend. The measured shape of the river bottom at the monitoring cross-section substantiates this theory. The river bottom is eroded at the outer bend (left side of the river) and probably deposition takes place in the inner bend. The differences in litter transport over the cross-section are, however, based on limited monitoring activities, especially for location 2.

According to the collected litter transport data for the different tides, significantly more litter items passed the sensor when the tide in the river is going from high to low. In other words, when water was flowing from inland to the sea. It may be possible that during high to low river tide, litter items present at floodplains enter the river and get transported, leading to an increase in transported litter as opposed to when the water is flowing from the sea to inland. On average, 19 and 38 items/hour were counted for incoming and outgoing river tide respectively. Compared to floating litter transport characteristics, obtained from van Calcar & van Emmerik (2019), the measured suspended litter load is less than the floating litter load for various rivers in Europe and Asia. However, no direct comparison can be made, since there is no information about the floating litter load in the Guadalete river present yet.

The results regarding the distribution of the detected litter particles over the river depth show approximately uniform distribution of the litter items. This indicates that a substantial part of riverine litter is transported underneath the water surface, and should, therefore, be taken into account when quantifying riverine litter transport.

5.

Synthesis from discussions

In this chapter, an overall discussion of the methods used and results obtained from the three different experiments is given.

In general, the accuracy of the results could be affected due to having to take screenshots of the sonar signal data. When using the Deeper CHIRP+ sonar data cannot be exported, leading to the need for image processing with the use of screenshots. In this thesis, MATLAB was used as image processing software, this could, however, also be performed with open-source programs such as Python and ImageJ.

Regarding the executed tests, different scanning beams were used during the performed methods. The controlled and semi-controlled tests were executed using the narrow beam. The narrow beam enables the highest scanning resolution, but the lowest spatial resolution compared to the medium and wide beams. During river monitoring in combination with nets and monitoring in the Guadalete river, the medium and wide beams were used. For the three different beams, blind zones are present at the water surface, at which no objects can be detected. The larger the scanning beam, the larger the blind zone. For the narrow, medium and wide beam of the Deeper CHRIP+, the blind zones are 15 cm, 60 cm and 80 cm, respectively. Regarding the controlled and semi-controlled tests, there is assured that the items passed the sensor below the blind zone. However, for the monitoring activities, it needs to be borne in mind that the collected data does not include the full river depth, due to the blind zones. For the sake of this research, investigating the possibilities of using echo sounding for suspended macroplastic detection, the methods used may be identified as primary tests, not including all specific facets. Furthermore, in this study, the scanning abilities using the different beams were not compared to each other, and could potentially be different. For example, signals of targets identified using the wide scanning beam, which has the lowest spatial resolution, could differ in shape and intensity compared when identified by using the smallest scanning beam, with the highest resolution.

According to the combination of tests executed, the following factors and findings have to be taken into account when estimating litter size using sonar. It became clear that the dimensions of the sonar signal are related to the actual size of the passing object. From the controlled tests, with spherical items, it was observed that a larger item results in a significant larger sonar signal than a smaller item. Moreover, the height of the sonar signal provides an estimation of the vertical dimension of the passing object, as indicated by the 1.5 L plastic bottle experiment. However, taking the results of the semi-controlled tests into account, the signal dimensions are likely to be influenced by object orientation and deformation. The data concerning the signal dimensions per tested object are inconsistent, probably caused by the rotation and deformation of the objects when passing the sensor. Transported suspended objects can move in a wide range of motion, passing the sensor each time differently orientated. Depending on the material properties, litter could also be deformed during transport, leading to uncertainties in estimating litter size from the sonar readings. Both orientation and deformation of the objects could be related to river flow conditions. When, for instance, turbulent flow is present, the influence of object orientation and deformation on the extend of the sonar signal could potentially be larger compared to uniform flow conditions.

Besides object orientation and deformation another possible cause for the deviations in the dimensions of the sonar signal has to do with the location an item is passing the scanning plane. Considering the top view of the scanned area, the xy-plane, an object can pass the scanned area in different ways. When an object travels through the centre of the plane, presumably a larger signal will be recorded compared to when an object only travels partially

through the plane. This could lead to differences in displayed object dimensions by the sonar. For single beam echosounders, it is not feasible to get an indication at which point in the xy-plane objects passed. Using a multibeam echosounder overcomes this issue, however, costs for these types of sensors are not comparable to the single beam echosounders.

Moreover, the different objects tested are represented by different sonar signals regarding size. Nonetheless, the differences in observed signal size between the tested objects are relatively small. Besides object orientation, deformation, and location in the xy-plane, flow velocity also affects the signal size. Items passing with high velocity are displayed significantly smaller than items passing with low velocities. Since the x-axis of the sonar readings represents time, correction for flow velocity is needed, in order to obtain a correct signal area. Flow velocities of 0.15 to 0.25 m/s were used in this research. The flow velocity upper limit of detection of objects using echo sounding was not considered in this study. However, also depending on the actual size of the objects, flow velocity could probably be a limiting factor for plastic detection using echo sounding.

Additionally, besides considering signal extent, signal intensities were also taken into account. According to sonar theory, signal intensities relate to signal strength. Signal strength can vary for different objects and is particularly determined by the material properties. If, not only size, but also material properties of the suspended litter can be estimated, a better understanding of the litter transport can be obtained. In this research, tests were performed for different types of plastics, and aluminium object. The obtained signal intensities of the executed experiments were compared to what would be expected according to material densities. A reasonable fit was found. In accordance with the expectations, the aluminium object corresponds to the highest signal intensity and the food wrappers with the lowest signal intensity. The relatively high signal intensity for the thin plastic bag is noticeable. This may be caused by air trapped in or air bubbles present on the material. Air reflects sound well and is probably the reason for the unexpected high signal intensity of the thin plastic bag. The presence of air bubbles may also have influenced the signal intensities of the other materials, however, the plastic bag was the only object in which air could be trapped. Although the found signal intensities do mainly correspond to the material properties, it is important to bear in mind that the differences in the obtained signal intensities for the different objects are small. With respect to the obtained data, no robust relation between signal intensity and material properties could be established.

In this research, sonar signal dimensions and intensity were considered separately, in order to examine different relationships. However, it could very likely be that these two aspects are linked. Objects with strong reflectivity may also lead to larger signals. Because different objects of different materials and sizes were used, this could not be investigated in this research. Recommendations on how to possibly deal with this are mentioned in Chapter 6. According to sonar theory, factors that could potentially influence both signal dimension and intensity, are water temperature, salinity and pressure. An increase in one of these factors causes an increase in soundwave velocity in water. Higher sound wave velocities lead to an increase in the accuracy of the sonar readings. During this research, the mentioned factors were not measured and could be a reason for the varying results. However, the estimated influence of these factors on the soundwave velocity, taking into account the circumstances during the measurements, is small. Additionally, a more likely factor that may have an impact on the accuracy of the sonar readings is turbidity. High turbidity induces noise in the sonar signal, possibly leading to inconsistency in sonar signals for the different measuring days.

When applying the obtained knowledge from the controlled and semi-controlled tests to the field, the following aspects should be taken into account when using echo sounding as a monitoring technique. As previously stated, the actual litter size is hard to estimate from the sonar readings because of object orientation and deformation. This implies an uncertainty when using the sensor for monitoring purposes. Moreover, river flow velocity is also an influencing factor when estimating litter size. Furthermore, signal intensities could provide an understanding of the material properties of monitored items. However, according to the obtained data during the experiments, the signal intensities do not significantly differ for the various tested objects. In addition, obtained data on litter transport depends on the chosen

beamwidth, leading to the presence of blind zones at the water surface. These aspects coincide with the findings concerning the river monitoring in combination with nets performed.

Finally, additional information on the ability of echo sounding for litter monitoring was obtained during the 18 hours of monitoring in the Guadalete river. From the data, it is clear that a distinct difference between fish and litter could be observed. When comparing the sonar signal data to fish finding theory, fish can be discarded from other objects by the specific shaped signal. However, this assumption is only based on fish finding theories and has not been validated. Moreover, the detected litter items in the Guadalete river were not uniformly distributed over the cross-section. The monitoring locations did not cover the entire cross-section. The monitoring activities were not evenly distributed over the different locations in the cross-section. Furthermore, a difference was observed in detected litter items for water flowing towards sea and water flowing inland. In general, significantly more items were found when water was flowing towards the sea. This may be caused by litter present on floodplains entering the river flow when the river tide is going from high to low. Besides the number of litter items transported by the river, the depth at which the items were present was also indicated. Results show an almost uniform distribution of the litter particles over the river depth. Taking into account the material properties of (suspended) plastics, it is likely that litter items are present at different depths based on their density. Additionally, turbulence, litter shape and vegetation may also influence the vertical location of the particles.

6.

Conclusions and Recommendations

Below, the conclusions and recommendations regarding the research conducted for this thesis are stipulated. The research aimed to investigate whether echo sounding could be used for suspended riverine macroplastic detection.

From the performed tests, both in a controlled environment as well as in a natural environment it can be concluded that an echosounder is able to detect suspended plastics under different circumstances. In natural rivers, where turbidity can be high and different types of litter are transported, medium-sized plastic objects give a distinct signal as compared to naturally occurring elements, such as fish.

Regarding estimating litter size from sonar readings, it can be concluded that several factors influence the sonar signal dimensions. When looking at spherical targets, it was observed that a larger item results in a larger sonar signal. The signal dimensions of non-spherical items, however, deviates when passing the sensor multiple times. This has most likely to do with object orientation and deformation. Besides object orientation and deformation, it was noticed that flow velocity also influences the dimensions of the sonar signal. For a higher flow velocity (0.25 m/s), the sonar signal is smaller than for lower flow velocity (0.15 m/s). At least one actual dimension of a passing object can be estimated by processing the sonar readings. However, due to object orientations and deformations, recorded dimensions may differ significantly. In order to indicate litter type, signal intensities may potentially be used to indicate material properties of the transported litter.

With regards to the suspended litter transport in the Guadalete river in Southern Spain, it was observed that the litter transport varies for outgoing and incoming tide, as well as over the width of the river. According to the observations, significantly more litter is transported when water is flowing from inland towards the sea than to water flowing inland from the sea. Moreover, the detected litter items are approximately uniformly distributed over the river depth. This illustrates the importance of monitoring riverine litter not only at the water surface or top layer but also at deeper layers in the river.

The ability to detect plastics by echo sounding enhances monitoring of transported litter over the full river depth. Moreover, in principle, no fixed structures are needed from which to deploy the sensor, which allows for flexible deployment. In general, monitoring suspended riverine macroplastics with echo sounding may provide a better understanding of suspended litter transport, from which prevention and mitigation strategies could be optimised.

Recommendations for further research and improvements in testing the ability of echo sounding (Deeper CHIRP+) for monitoring macroplastics, according to this research, are stated below. First of all, testing more items for a wider range in size could provide more insight. Especially including smaller items, to check the limits of litter detection concerning litter size. Moreover, to make sure the depth of objects passing the sensor is not influencing the sonar readings, additional tests should be performed for a wider range of depths and more repetition. To examine whether the sensor can still detect items in fast-flowing rivers, testing for higher flow velocities should be performed. In this research, the ability to detect litter was only tested up to a velocity of 0.25 m/s.

Additionally, an important point concerning estimating actual object size from sonar readings is to differentiate between signal dimension and reflectance. To separate signal size from signal reflectance, objects of the same material properties but different sizes could be tested, in combination with testing similar objects of different materials. Additionally, flow velocity

appeared to influence the sonar signal dimensions and should be taken into account when estimating litter size. Furthermore, the location in the xy-plane where the objects pass the scanning beam may also have an impact on the signal displayed. However, when using a single beam echosounder, no information on the location in the xy-plane of an object passing the scanning beam can be provided.

Furthermore, the nuance of the research could be increased by looking into the difference in accuracy between scanning beams. Additionally, the presence of blind zones should be considered when choosing an appropriate scanning beam. Besides, the possible influence of water temperature, salinity, pressure and turbidity on the accuracy of the sonar readings, should be elucidated.

Besides, when using the Deeper CHIRP+ for monitoring riverine macroplastics, automated sonar signal analysis is recommended. To be able to automatically count passing litter items would be time-saving and improve the applicability of this monitoring method. A possible solution might be using particle counting or tracking to determine litter transport loads.

When considering using a different single beam echosounder than the one used in this study, choosing a sensor for which the sonar data can be exported is advisable. In this way, signal image analysis would not be necessary and the accuracy of test results will likely increase. It could also be interesting to see whether other types of echosounders perform better. For example, using a multibeam or side scan sonar. These types of sensors are more robust, but also more expensive compared to single beam sonars.

With regards to monitoring in natural rivers, it could be interesting to add floating litter monitoring, in order to observe possible differences in floating and suspended litter transport. To validate sonar readings during monitoring, the sensor could be used in front of nets, as was done in this research. However, when doing so, it is recommendable to empty the net when an item passes the sonar. This enables directly relating the sonar signal to the item caught with the net. This is, however, labour intensive. Lastly, more research to the distribution of litter particles over the river depth is needed. According to this research, the transported riverine litter is distributed uniformly over the river depth. To validate and support this finding, extensive research on the distribution over litter items over the river depth, in various rivers and under different circumstances, should be executed. Most importantly, suspended litter should not be left out when quantifying riverine litter transport.

Bibliography

Ainslie, M. A. (n.d.). *PRINCIPLES OF SONAR PERFORMANCE.*

Ayuntamiento de Jerez. (2019). El Río Guadalete en el Planeamiento Urbanístico. Retrieved October 10, 2019, from https://www.jerez.es/webs_municipales/medio_ambiente/zonas_verdes/rio_guadalete /

Blomquist, W., Giansante, C., Bhat, A., & Kemper, K. (2005). Institutional and policy analysis of river basin management. The Guadalquivir River Basin, Spain. *Water*, (April), 1–40. https://doi.org/10.1029/2003WR002726.1

Brown. (2019). The properties of SOUND WAVES. Retrieved November 12, 2019, from http://www.docbrown.info/ephysics/wavesound.htm

Cannas, S., Fastelli, P., Guerranti, C., & Renzi, M. (2017). Plastic litter in sediments from the coasts of south Tuscany (Tyrrhenian Sea). *Marine Pollution Bulletin*, *119*(1), 372–375. https://doi.org/10.1016/j.marpolbul.2017.04.008

Chauhan, N. S. (2019). Introduction to Image segmentation with K-Means clustering. Retrieved November 18, 2019, from https://towardsdatascience.com/introduction-to-image-segmentation-with-k-means-clustering-83fd0a9e2fc3

Christ, R. D., & Wernli, R. L. (2014). Sonar. In *The ROV Manual.* https://doi.org/10.1016/b978-0-08-098288-5.00015-4

Deeper. (2019). No Title. Retrieved November 5, 2019, from https://deepersonar.com/nl/nl_nl

Educba. (2019). RGB Color Model. Retrieved November 17, 2019, from https://www.educba.com/rgb-color-model/

European Commission. (2018). *EU plastics-strategy Jan 2018.* https://doi.org/10.1021/acs.est.7b02368

European Parliament. (2015). *DIRECTIVE (EU) 2015/720 OF THE EUROPEAN PARLIAMENT AND OF THE COUNCIL of 29 April 2015 amending Directive 94/62/EC as regards reducing the consumption of lightweight plastic carrier bags. 2014*(April 2014), 11–15.

European Parliament. (2019). Parliament seals ban on throwaway plastics by 2020. Retrieved October 10, 2019, from https://www.europarl.europa.eu/news/en/press-room/20190321IPR32111/parliament-seals-ban-on-throwaway-plastics-by-2021

Garbade, M. J. (2018). Understanding K-means Clustering in Machine Learning. Retrieved November 18, 2019, from https://towardsdatascience.com/understanding-k-means-clustering-in-machine-learning-6a6e67336aa1

Gasperi, J., Dris, R., Bonin, T., Rocher, V., & Tassin, B. (2014). Assessment of floating plastic debris in surface water along the Seine River. *Environmental Pollution (Barking, Essex : 1987)*, *195*, 163–166. https://doi.org/10.1016/j.envpol.2014.09.001

González, D., Hanke, G., Tweehuysen, G., Bellert, B., Holzhauer, M., Palatinus, A., … Oosterbaan, L. (2016). Riverine Litter Monitoring - Options and Recommendations - Thematic Report. In *JRC Scientific and Technical Reports.* https://doi.org/10.2788/461233

Hedquist, K. (2016). Understanding Sonar Learn how to understand 2D, Downscan and SideScan Sonar. Retrieved November 13, 2019, from https://www.youtube.com/watch?v=2Q9izOwp1aU%0D

Hendricks, J. (2018). Changing to Chirp Sonar. Retrieved November 12, 2019, from https://www.saltwatersportsman.com/chirp-sonar-versus-traditional-sonar/

Hofman, J. (2017). Viral seahorse photo - Indonesia. Retrieved October 10, 2019, from https://www.justin-hofman.com/viral-seahorse-print

Hohenblum, P., Frischenschlager, H., Reisinger, H., Konecny, R., Uhl, M., Mühlegger, S., … Rindler, R. (2015). *Plastik in der Donau.*

Hritik, R. (2019). MATLAB RGB image representation. Retrieved November 18, 2019, from https://www.geeksforgeeks.org/matlab-rgb-image-representation/

Jambeck, J. R. (2015). Plastic waste inputs from land into the ocean. *Science*, (September 2014), 1655–1734. https://doi.org/10.1017/CBO9781107415386.010

Lebreton, L. C. M., Van Der Zwet, J., Damsteeg, J. W., Slat, B., Andrady, A., & Reisser, J. (2017). River plastic emissions to the world's oceans. *Nature Communications*, *8*, 1–10. https://doi.org/10.1038/ncomms15611

Lechner, A., Keckeis, H., Lumesberger-Loisl, F., Zens, B., Krusch, R., Tritthart, M., … Schludermann, E. (2014). The Danube so colourful: A potpourri of plastic litter outnumbers fish larvae in Europe's second largest river. *Environmental Pollution*, *188*, 177–181. https://doi.org/10.1016/j.envpol.2014.02.006

Liedermann, M., Gmeiner, P., Pessenlehner, S., Haimann, M., Hohenblum, P., & Habersack, H. (2018). A methodology for measuring microplastic transport in large or medium rivers. *Water (Switzerland)*, *10*(4), 1–12. https://doi.org/10.3390/w10040414

Lurton, X., & Lamarche, G. (2015). Backscatter measurements by seafloor-mapping sonars. Guidelines and Recommendations. *Geohab Report*, (May), 200. Retrieved from http://geohab.org/wp-content/uploads/2013/02/BWSG-REPORT-MAY2015.pdf

Mackenzie, K. V. (1981). Nine-term equation for the sound speed in oceans. *The Journal of the Acoustical Society of America*, *70*(3), 807–812.

Más Spanje. (2019). Langs de Guadalquivir (Córdoba). Retrieved October 10, 2019, from https://www.masspanje.nl/autoroutes-cordoba%0D

Morritt, D., Stefanoudis, P. V., Pearce, D., Crimmen, O. A., & Clark, P. F. (2014). Plastic in the Thames: A river runs through it. *Marine Pollution Bulletin*, *78*(1–2), 196–200. https://doi.org/10.1016/j.marpolbul.2013.10.035

Outdoor Nirvana. (2019). Using a Fish Finder. Retrieved November 13, 2019, from https://www.outdoornirvana.com/best-fish-finders/using-a-fish-finder/

Panbo. (2019). Discover how the Furuno DFF3D mult-beam sonar works inside TZ Professional v3.3. Retrieved November 13, 2019, from https://www.panbo.com/discover-how-the-furuno-dff3d-multi-beam-sonar-works-inside-tz-professional-v3-3/#lightbox-gallery-0/0/%0D

Plastics – the Facts 2019. (2019).

PlasticsEurope2018. (2018). *71*(1–2), 299–306. https://doi.org/10.1016/j.marpolbul.2013.01.015

Schmidt, C., Krauth, T., & Wagner, S. (2017). Export of Plastic Debris by Rivers into the Sea. *Environmental Science and Technology*, *51*(21), 12246–12253. https://doi.org/10.1021/acs.est.7b02368

Tramoy, R., Gasperi, J., Dris, R., Colasse, L., Fisson, C., Sananes, S., … Tassin, B. (2019). Assessment of the Plastic Inputs From the Seine Basin to the Sea Using Statistical and Field Approaches. *Frontiers in Marine Science*, *6*(April), 1–10. https://doi.org/10.3389/fmars.2019.00151

University of Rhode Island. (2019). How is sound used to locate fish? Retrieved November 13, 2019, from https://dosits.org/people-and-sound/fishing/how-is-sound-used-to-locate-fish/%0D

van Calcar, C. J., & van Emmerik, T. H. M. (2019). Abundance of plastic debris across European and Asian rivers. *Environmental Research Letters*, *14*(12), 124051. https://doi.org/10.1088/1748-9326/ab5468

van der Wal, M., van der Meulen, M., Tweehuijsen, G., Peterlin, M., Palatinus, A., Kovač Viršek, M., … Kržan, A. (2015). Identification and Assessment of Riverine Input of (Marine) Litter. *Final Report for the European Commission DG Environment under Framework Contract No ENV.D.2/FRA/2012/0025*, (April), 1–208. Retrieved from http://mcc.jrc.ec.europa.eu/document.py?code=201606244356

van Emmerik, T., Kieu-Le, T.-C., Loozen, M., van Oeveren, K., Strady, E., Bui, X.-T., … Tassin, B. (2018). A Methodology to Characterize Riverine Macroplastic Emission Into the Ocean. *Frontiers in Marine Science*, *5*(October), 1–11. https://doi.org/10.3389/fmars.2018.00372

van Emmerik, T., & Schwarz, A. (2019). *Plastic debris in rivers*. (October 2019). https://doi.org/10.1002/wat2.1398

Wikimedia Commons. (2019). RGB color model. Retrieved November 17, 2019, from https://commons.wikimedia.org/wiki/File:RGB_color_model.svg

Yngstr's Weblog. (2008). Acoustical Motion Sensors. Retrieved November 7, 2019, from https://yngstr.wordpress.com/2008/01/11/acoustical-motion-sensors/

Zaat, L. (2020). Below the surface. Retrieved February 5, 2020, from http://resolver.tudelft.nl/uuid:1b40f6c9-7532-4033-9e13-d5efb927f9ac

A) Controlled tests in artificial environment

Below, in Figure 54, the actual test setup used in the Kerkpolderbad in Delft is presented. The steel bars used as weights were present at the bottom of the pool. Lines attached to the weight and the floats on top of the water surface served as a framework to attach the balloons and sensor to. The sensor was fixed at the water surface in the middle of the framework. In the figure below, the large balloon is attached to the line framework at 1 m depth.
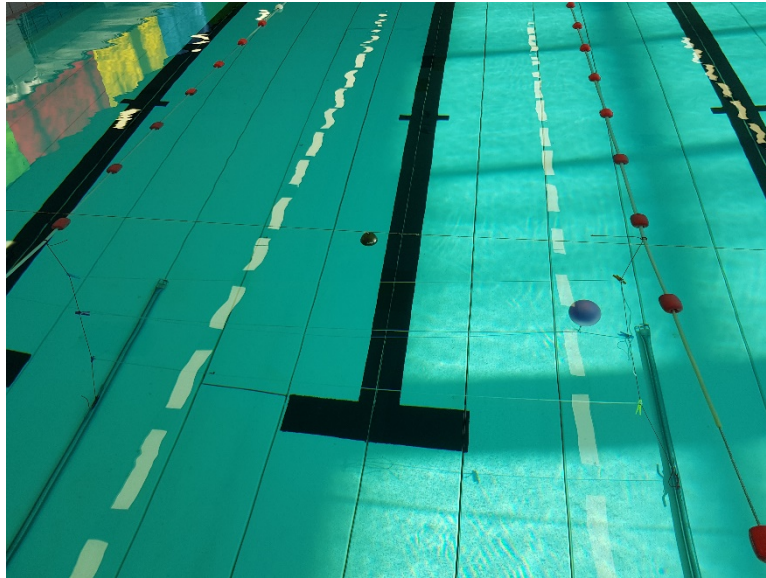

Figure 54: Experimental setup, controlled tests artificial environment, Kerkpolder swimmingpool, Delft

The actual balloons used during the controlled tests are shown in Figure 55. The small and large balloon of 8 and 15 cm diameter respectively were attached to the framework at 0.5 and 1 m depth and dragged underneath the sensor.

Figure 55: Spherical objects, balloons (8 cm, 15 cm) used for the controlled tests in the artificial environment.

B) Semi-controlled tests in natural environment

The targets used for the semi-controlled tests in the Rio de San Pedro are displayed in Table 12. Eight different targets of different size and material property were used.

Table 12: Target items used for the semi-controlled tests in the natural environment.

1	2	3	4
Height (cm): 12.5 Width (cm): 6.5-9 (b-t)	Height (cm): 38 Width (cm): 26	Height (cm): 12 Width (cm): 6.5	Height (cm): 23 Width (cm): 6
5	6	7	8
Height (cm): 27 Width (cm): 8.5	Height (cm): 19 Width (cm): 6	Height (cm): 12.5 Width (cm): 4.5	Height (cm): 16.5 Width (cm): 9 Depth (cm): 6

C) River monitoring

The items caught by the two (surface and bottom) nets during the three-hour monitoring activity in the Guadalquivir river are shown in Figure 56 and Figure 57.

Figure 56: Litter caught in the surface net during the monitoring activity in the Guadalquivir river.

Figure 57: Litter caught in the bottom net during the monitoring activity in the Guadalquivir river.

D) MATLAB scripts

The scrips written for the sonar signal image analysis in MATLAB are provided below.

Script used for K-Means pixel clustering:

```matlab
function [BW,maskedImage] = segmentImage_auto1(my_images)
%segmentImage Segment image
% Convert RGB image into L*a*b* color space.
X = rgb2lab(my_images);

% Auto clustering
sz = size(X);
im = single(reshape(X,sz(1)*sz(2),[]));
im = im - mean(im);
im = im ./ std(im);
s = rng;
rng('default');
L = kmeans(im,2,'Replicates',2);
rng(s);
BW = L == 2;
BW = reshape(BW,[sz(1) sz(2)]);

% Create masked image.
maskedImage = my_images;
maskedImage(repmat(~BW,[1 1 3])) = 0;
end
```

Script used for calculating signal width, height, and area:

```matlab
clc;
image_folder='C:\Users\sophie\Documents\MATLAB\Zwembad_diepte1_grote_ballon_langzaam';
filenames = dir(fullfile(image_folder, '*.PNG')) %read all images with specified extention, png in this case
total_images = numel(filenames); %count total number of images present in that folder
area_seg_images = zeros(1,total_images);%avoid overwriting variable
binaryImage = zeros(1,total_images);
MaxNumOnesColumn = zeros(1,total_images);
MaxNumOnesRow = zeros(1,total_images);
AvNumOnesColumn = zeros(1,total_images);
AvNumOnesRow = zeros(1,total_images);

for n = 1:total_images
    f = fullfile(image_folder, filenames(n).name); %it will specify images names with full path and extension
    my_images = imread(f); %read images
    [BW,maskedImage] = segmentImage_auto1(my_images);
    area_seg_images(n) = bwarea(segmentImage_auto1(my_images));
    binaryImage = segmentImage_auto1(my_images);
    %figure(n) %used tat index n so old figures are not over written by new figures
    %imshow(binaryImage) %show all images

    numberOfOnesPerColumn = sum(binaryImage, 1); %height values
    numberOfOnesPerRow = sum(binaryImage, 2); %width values

    MaxNumOnesColumn(n) = max(sum(binaryImage,1)); %max height
    MaxNumOnesRow(n) = max(sum(binaryImage,2)); %max width

    numberOfOnesPerColumn(numberOfOnesPerColumn ==0) = NaN; %set zero height values to NaN
    numberOfOnesPerRow(numberOfOnesPerRow ==0) = NaN; %set zero width values to Nan

    AvNumOnesColumn(n) = nanmean(numberOfOnesPerColumn, 'all'); %average height
    AvNumOnesRow(n) = nanmean(numberOfOnesPerRow, 'all'); %average width
end
```

Script used for splitting RGB colour channels and calculating mean, min, max, and std RGB pixel values. Besides, the number of RGB pixels present in the images is determined.

```matlab
clc;
image_folder='C:\Users\sophie\Documents\MATLAB\Guadalquivir_net';
filenames = dir(fullfile(image_folder, '*.PNG')) %read all images with specified extention, png in this case
total_images = numel(filenames); %count total number of images present in that folder

mean_red_pix = zeros(1,total_images);%avoid overwriting variable
mean_green_pix = zeros(1,total_images);
mean_blue_pix = zeros(1,total_images);

min_red_pix = zeros(1,total_images);%avoid overwriting variable
min_green_pix = zeros(1,total_images);
min_blue_pix = zeros(1,total_images);

max_red_pix = zeros(1,total_images);%avoid overwriting variable
max_green_pix = zeros(1,total_images);
max_blue_pix = zeros(1,total_images);

std_red_pix = zeros(1,total_images);%avoid overwriting variable
std_green_pix = zeros(1,total_images);
std_blue_pix = zeros(1,total_images);

Num_red_pix = zeros(1,total_images);%avoid overwriting variable
Num_green_pix = zeros(1,total_images);
Num_blue_pix = zeros(1,total_images);

for n = 1:total_images
    f = fullfile(image_folder, filenames(n).name); %it will specify images names with full path and extension
    my_images = imread(f); %read images

    %Split channels (R-G-B)
    redChannel = my_images(:,:,1); % Red channel (in grayscale)
    greenChannel = my_images(:,:,2); % Green channel (in grayscale)
    blueChannel = my_images(:,:,3); % Blue channel (in grayscale)

    todoublered = double(redChannel);
    todoublered(todoublered ==0) = NaN;%set black background values to NaN
    todoublegreen = double(greenChannel);
    todoublegreen(todoublegreen ==0) = NaN;%set black background values to NaN
    todoubleblue = double(blueChannel);
    todoubleblue(todoubleblue ==0) = NaN;%set black background values to NaN

    Num_red_pix(n) = sum(~isnan(todoublered), 'all'); %calculates number of non NaN elements, for red channel
    Num_green_pix(n) = sum(~isnan(todoublegreen), 'all');
    Num_blue_pix(n) = sum(~isnan(todoubleblue), 'all');

    mean_red_pix(n) = nanmean(todoublered, 'all'); %calculates mean of all non NaN values
    mean_green_pix(n) = nanmean(todoublegreen, 'all');
    mean_blue_pix(n) = nanmean(todoubleblue, 'all');

    min_red_pix(n) = nanmin(todoublered,[], 'all'); %calculates min of all non NaN values
    min_green_pix(n) = nanmin(todoublegreen,[], 'all');
    min_blue_pix(n) = nanmin(todoubleblue,[], 'all');

    max_red_pix(n) = nanmax(todoublered,[], 'all');%calculates max of all non NaN values
    max_green_pix(n) = nanmax(todoublegreen,[], 'all');
    max_blue_pix(n) = nanmax(todoubleblue,[], 'all');

    std_red_pix(n) = nanstd(todoublered,0, 'all'); %calculates std of all non NaN values
    std_green_pix(n) = nanstd(todoublegreen,0, 'all');
    std_blue_pix(n) = nanstd(todoubleblue,0, 'all');

end
```